# "EFFECT OF PRESTRESS LEVEL ON BEAMS RETROFITTED WITH PRESTRESSED FRP SHEETS"

A Thesis report submitted in the partial fulfillment

of the requirement for the award of degree

of

**MASTERS OF ENGINEERING**

**IN**

**STRUCTURAL ENGINEERING**


Submitted By:-

**Raju Sharma**

**Roll No.801122015**

**Under the Supervision of**

**Dr. Prem Pal Bansal**

**(Assistant Professor, CED)**

**Thapar University**

**Patiala**



**DEPARTMENT OF CIVIL ENGINEERING**

**THAPAR UNIVERSITY, PATIALA-147004**


**JANUARY – JUNE (2013)**

# CERTIFICATE

This is to certify that the thesis titled, **"EFFECT OF PRESTRESS LEVEL ON BEAMS RETROFITTED WITH PRE-STRESSED FRP SHEETS"** in partial fulfillment of the award of degree of **MASTER OF ENGINEERING (STRUCTURAL ENGINEERING)** in the **Department Of Civil Engineering, Thapar University,** is a bonafied work carried out by him under my guidance and supervision and that no part of this thesis report has been submitted for the award of any other degree.

Dr. Prem Pal Bansal
Assistant Professor
Thapar university
Patiala

15/7/13

Dr. Naveen Kawatra
Associate Professor & Head of Department
Department of Civil Engineering
Thapar University
Patiala

Dr. S K Mohapatra
Dean of Academic Affairs
Thapar University
Patiala

# ACKNOWLEDGEMENT

The thesis period has a lots of difficulties, new experiences that how to overcome these difficulties, continuous endeavors and their results. Besides of that we need a continuous motivation and experienced guidance to achieve the desired result.

I would like to thank my guide Dr. Prem Pal Bansal (Assistant Professor, Thapar University) for his immense profundity regarding research work and his continuous technical and motivational support for the completion of this thesis.

The successful completion of this thesis will not be completed until I give my gratitude to all my faculty member, teaching and non teaching staff and my friends Miss Rinki Verma, Mr Jatinder Malhotra, Mr Pardeep Sharma who helped me by heart to complete this thesis.

Date- Raju Sharma

Place:

# ABSTRACT

The Retrofitting is a technique of strengthening the existing structures which are unable to take the unpredicted loads and deteriorated due to environmental effect. This technique has been effectively applied on the existing structures like buildings, dams, bridges etc. There is a various existing techniques of retrofitting which are section enlargement (jacketing), bonded steel plates, strengthening with FRP composite sheets. A lot of research has been carried out for above retrofitting techniques. From all the above techniques, FRP is the most effectively used for the retrofitting. The advantages of resistance to corrosion and higher specific strength make this material ideal for reinforcing existing structures.

For retrofitting the existing structures, FRP can be used by various techniques such as FRP laminates, FRP non prestressed sheets, FRP prestressed sheets, FRP wrapping and FRP reinforcement also. The amount of research conducted on retrofitting by prestressed FRP sheet is quite less. So in this thesis, the effect of different prestresse levels of FRP sheets on beams have been carried out.

## CONTENTS

## LIST OF FIGURE

## LIST OF TABLE

# CHAPTER -1

# INTRODUCTION

## 1.1 General

During the service life of reinforced cement concrete structure, it frequently need a modification and improvement in their performance. The main factors are change in their use, new design standards, deterioration due to corrosion in the steel caused by exposure to an aggressive environment and accident events such as earthquake

In such state of affairs there are two feasible solutions;

1 Replacement

2 Retrofitting

Full structure replacement have determinate disadvantage such as high cost for material and labour, long time requirement to make it usable , a stronger environment impact, utilization of waste material.

In the last decade retrofitting of the damaged or partially damaged structures has been increased. The development in retrofitting techniques of structures are essential due to many reasons, such as to make the structures fit for additional loading requirements, additional safety aspect of non-engineered buildings, update the building to current seismic codes etc. Existing retrofitting techniques are

- Section enlargement (jacketing)
- Bonded steel plates,
- Strengthening with FRP composite sheets.

Among all of above, Fiber Reinforced Polymer (FRP) composite sheets are more popular for retrofitting of concrete structure. Fiber Reinforced Polymer (FRP) is a relatively new class of composite material, manufactured from fibers and resins. It has proven efficient and economical for the development and repair of new and deteriorating structures in civil engineering. The mechanical properties of FRP make them ideal for widespread applications in construction worldwide. Although strengthening with FRP composite sheets have inherent demerits, such as

high cost, need of sophisticated instruments, surface preparation, occurrence of debonding failure, low benefit cost ratio etc. (Kothandaraman et al.2010).

Despite of that FRP materials provide several advantages over traditional construction materials such as high strength, high fatigue strength, light in weight, high durability, high strength to weight ratio, good resistance to chemical as compared to steel, have non magnetic and non conductive properties which is much more beneficial for the structure as compare to its demerits[18]. Carbon Fiber Reinforced Polymer (CFRP) is the most leading choice among from Fiber Reinforced Polymer due to its improved mechanical properties.

## 1.2 Commonly Used FRP are as Under

1) Carbon fiber reinforced polymer

2) Glass fiber reinforced polymer

3) Aramid Fiber reinforced polymer

### 1.2.1 Carbon Fiber Reinforced Polymer

CFRP is a most attractive choice of researchers for rehabilating the damaged structure due to its improved mechanical properties. Carbon fiber is woven into a textile material and resin such as epoxy resin is applied and allowed to cure. Carbon fibers are manufactured in diameters ranging from 9 to 17 μm. These fibers wound into larger threads for transportation and further production processes (Erhard & Gunter 2006). Further production processes include weaving or braiding into carbon fabrics, cloths and mats. The resulting material that is very strong as it has the best strength to weight ratio of all construction materials. It is an improvement on glass fiber reinforced plastic, although much more expensive.

**Fig-1.1 Carbon Fiber Reinforced Polymer**

### 1.2.2 Glass Fiber Reinforced Polymer

Fiber glass is, as its name implies, glass that has been spun into the form of fibers. Fiberglass is not as strong or stiff as carbon fibers, but it has characteristics that make it desirable in many applications. Fiberglass is non-conductive (i.e. an insulator) and it is generally invisible to most types of transmissions. This makes it a good choice when dealing with electrical or broadcast applications. There are five major types of fiberglass.

**A-glass (alkali glass)** which has good chemical resistance, but lower electrical properties.

**C-glass (chemical glass)** which has very high chemical resistance.

**E-glass (electrical glass)** which is an excellent insulator and resists attacks from water

**D-glass (dielectric glass)** which has the best electrical properties but lacks in mechanical properties when compared to E and S glass.

**E-glass and S-glass** are, by far, the most common types found in composites. These types have good combinations of chemical resistance, mechanical properties and insulating properties. Of the two, E-glass offers the more attractive economics, and S-glass offers better mechanical performance.

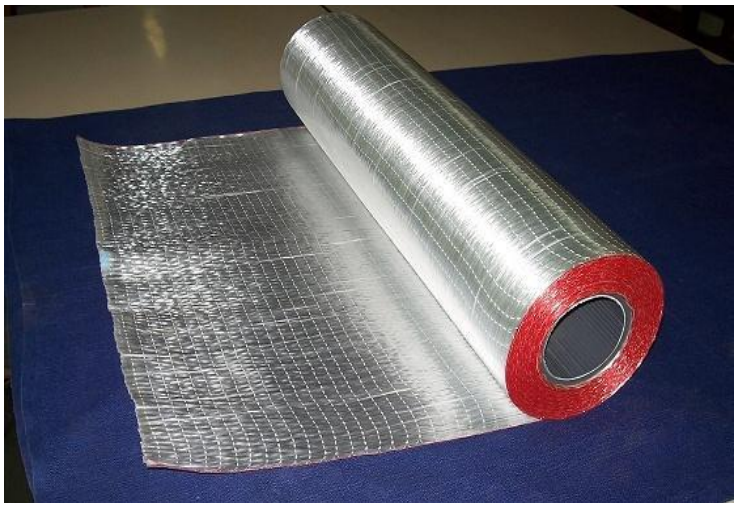

**Fig- 1.2 Glass Fiber Reinforced Polymer**

### 1.2.3 Aramid Fiber Reinforced Polymer

These are synthetic organic fibers consisting of aromatic polyamides. The aramid fibers have excellent fatigue and creep resistance. Although there are several commercial grades of aramid fibers available, the two most common ones used in structural applications are Kevlar 29 and Kevlar 49. The Young's Modulus curve for Kevlar 29 is linear to a value of 83 GPa but then becomes slightly concave upward to a value of 100 GPa at rupture; whereas, for Kevlar 49 the curve is linear to a value of 124 GPa at rupture (see Table ). As an anisotropic material, it's transverse and shear modulus are an order of magnitude less than those in the longitudinal direction. The fibers can have difficulty achieving a chemical or mechanical bond with the resin.

**Table-1.1 Properties of Aramid Fiber (ZWEBEN, C. 1989)**

| Typical Properties | Kevlar 29 | Kevlar 49 |
|---|---|---|
| Density (g/cm$^3$) | 1.44 | 1.44 |
| Young's Modulus (GPa) | 83/100 | 124 |
| Tensile Strength (GPa) | 2.27 | 2.27 |
| Tensile Elongation (%) | 2.8 | 1.8 |

## 1.3 Manufacturing Methods for FRP Composites

(1) Hand lay-up (2) Compression molding (3) Pultrusion (4) Resin transfer molding

(5) Injection molding (6) Filament winding

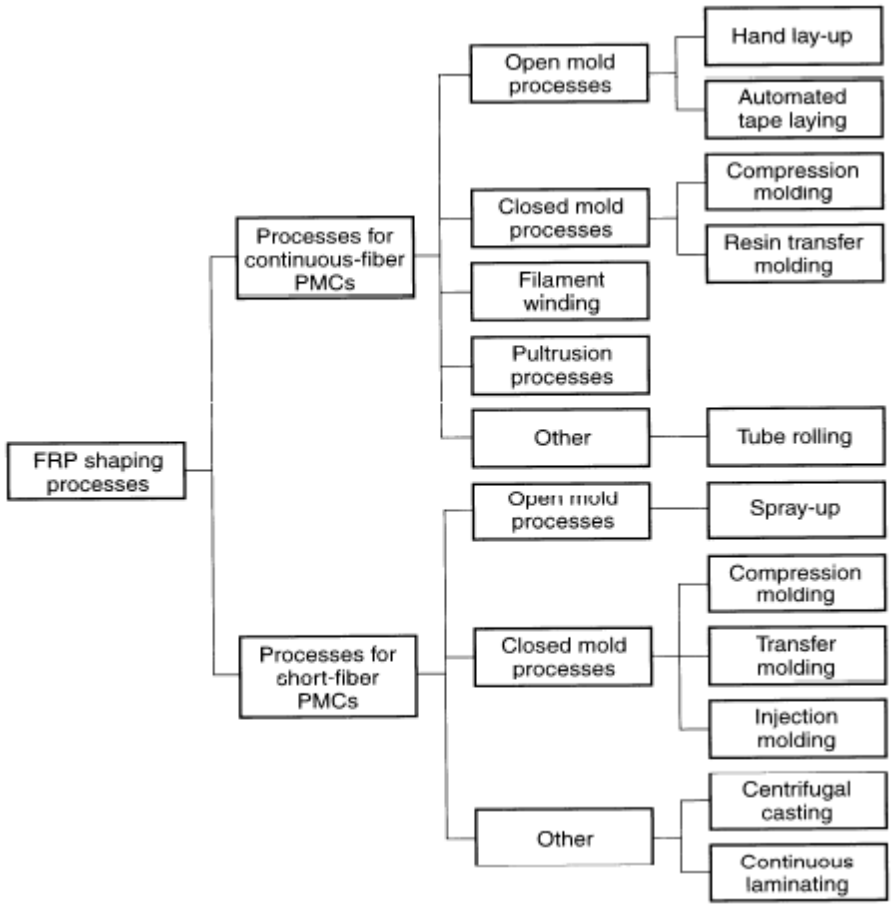


**Fig-1.3 Classification of FRP Processes**

### 1.3.1 Hand Lay-up

In this process resins are impregnated by hand into fibers which are in the form of woven, knitted, stitched or bonded fabrics. Hand lay up process usually accomplished by rollers or brushes. An increasing use of nip-roller type impregnators for forcing resin into the fabrics by means of rotating rollers and a bath of resin. Laminates then, are left to cure under standard atmospheric conditions. Epoxy ,polyester, vinylester, phenolic can be used in the form of resins and any type of fibers can be used. Although heavy aramid fabrics can be hard to wet-out by

hand. Typical application of hand lay up process is in wind turbine ,production boats, architectural mouldings. The schematic diagram below showing the Hand lay up process.

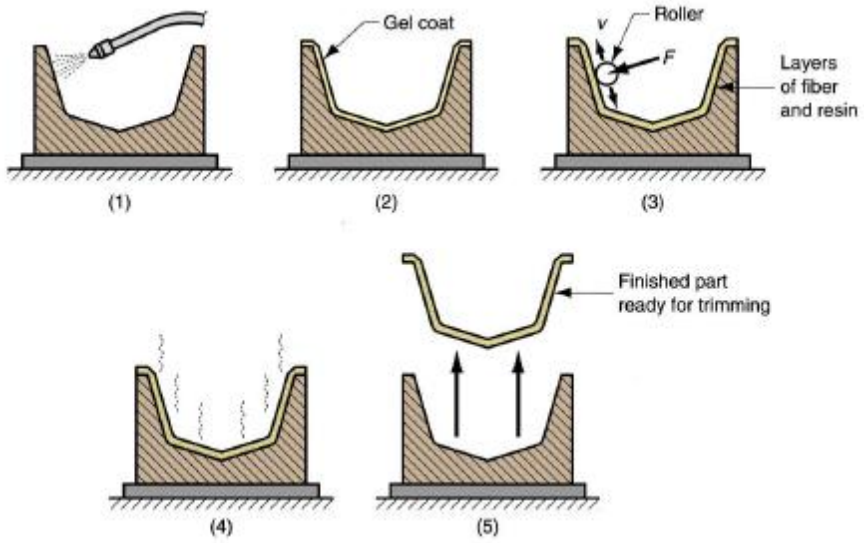


**Fig 1.4 Schematic diagram of Hand Lay up**

**(1) mold is treated with mold release agent; (2) thin gel coat (resin) is applied, to the outside surface of molding; (3) when gel coat has partially set, layers of resin and fiber are applied, the fiber is in the form of mat or cloth; each layer is rolled to impregnate the fiber with resin and remove air; (4) part is cured; (5) fully hardened part is removed from mold.**

### 1.3.2 Compression Molding

The compression molding method generally include the steps of

1) Placing a quantity of bulk molding compound into a female die of a mould. the bulk molding compound is a mixture which include pre ceramic
2) Pressing a male die of the mould into a female die so as to displace the bulk molding compound throughout a cavity formed between the male and female die. The wall of the cavity form the exterior surface FRCMC part being molded
3) Heating the mould at a temperature and for a time associated pre-ceramic resin which polymerizes the resin to form a fiber reinforced polymer composite structure
4) Removing the polymerized composite structure from the mould

5) Heating the polymerized composite structure at a temperature and a time associated with the pre-cremic resin which pyrolyzes it to form a FRCMC structure. (Atumer et al.1998)

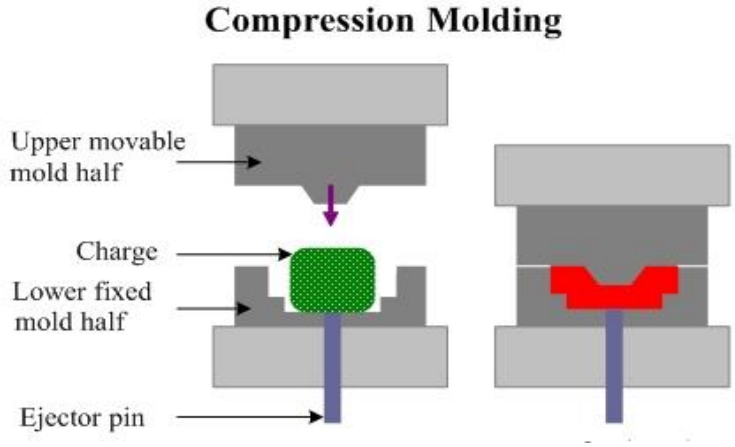


. **Fig-1.5 Compression Molding process**

### 1.3.3 Pultrusion

Pultrusion in a continuous manufacturing process utilized to make pultruded profiles with constant cross-sections whereby reinforcements, in the form of roving and mats, are saturated with resin and guided into a heated die. Once in the die, the resin undergoes a curing process known as polymerization. The once resin saturated reinforcements exit the die in a solid state and in the form of the cross section of the die. The pultrusion process requires little labor and is ideal for mass production of constant cross section profiles. Figure 1.6 shows the complete description of pultrusion process.

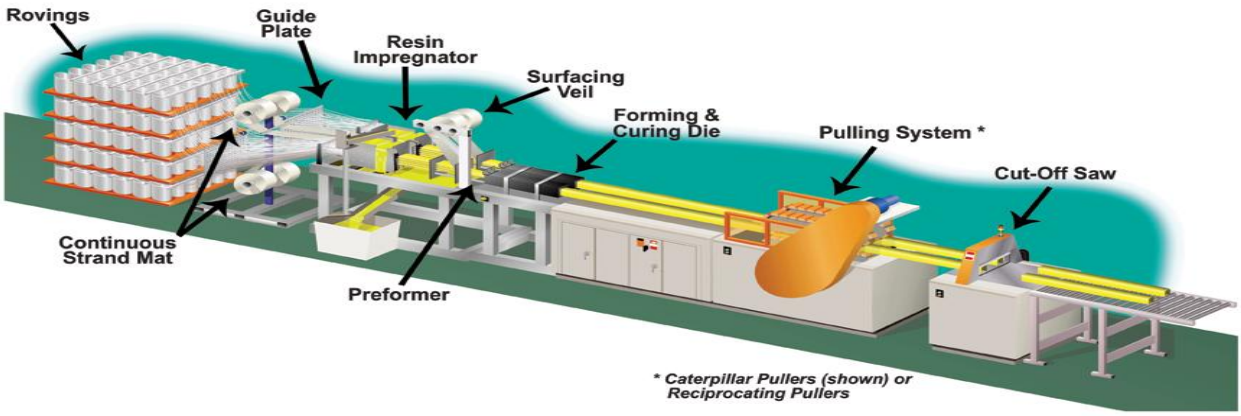


**Fig-1.6 pultrusion process**

### 1.3.4 Resin Transfer Molding

Fabrics are placed into a mold and wet resin is infused in-process. Resin is typically pressurized and forced into a cavity which is under vacuum in the RTM process. Resin is entirely pulled into cavity under vacuum in the VARTM process.

- Either one-sided tooling or matched tooling.
- Good process when dimensional tolerances are important for two surfaces
- Requires special consideration to assure thorough stauration of reinforcement material. "Race tracking" is a common problem where some areas are left unsaturated. Difficult to detect without expensive equipment.
- Common parts include boat hulls and aerospace structures·

### 1.3.5 Injection molding

Injection molding is widely used to process short fibre reinforced thermoplastics. Injection molding consists of high pressure injection of the raw material into a mold which shapes the polymer into the desired shape. No chemical reaction occurs during the molding process

### 1.3.6 Filament winding

Resin-impregnated continuous fibers are wrapped around a rotating mandrel that has the internal shape of the desired FRP product; the resin is then cured and the mandrel removed The fiber rovings are pulled through a resin bath immediately before being wound in a helical pattern onto the mendral The operation is repeated to form additional layers, each having a criss-cross pattern with the previous, until the desired part thickness has been obtained

## 1.4 Mechanical Properties of Fiber Reinforced Polymer

FRP is the most preferred choice for the structure applications due to its higher mechanical properties over other material. Figure 1.7 shows the stress strain behavior of FRP and Mild Steel. The kink in a Mild steel shows the limit of elastic behavior of steel and commencement of plastic behavior but in all types of FRP the behavior is fully elastic up to end. During Failure of FRP sudden transfer of load from FRP to Structure element is a anxious state under discussion. Table

1.2 shows the strength and stiffness values by which adoption of material for the particular job become easier.

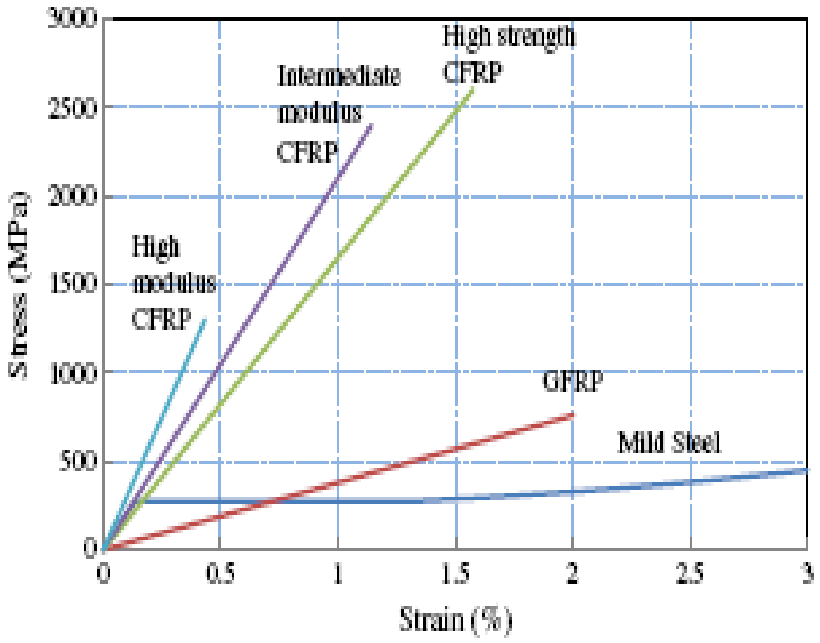


**Fig-1.7 Typical FRP and mild steel stress–strain curves (Teng et al 2012)**

**Table-1.2 Typical strength and stiffness values for materials used in retrofitting, (Piggott, M. 2002)**

| Material | Tensile strength (MPa) | Modulas of Elasticity (GPa) | Density ($Kg/m^3$) | Modulas of Elasticity to Density ($Mm^2/s^2$) |
|---|---|---|---|---|
| Carbon | 2200-5600 | 240-830 | 1800-2200 | 130-380 |
| Aramid | 2400-3600 | 130-160 | 1400-1500 | 90-110 |
| Glass | 3400-4800 | 70-90 | 2200-2500 | 31-33 |
| Epoxy | 60 | 2.5 | 1100-1400 | 1.8-2.3 |
| CFRP | 1500-3700 | 160-540 | 1400-1700 | 110-320 |
| Steel | 280-1900 | 190-210 | 7900 | 24-27 |

## 1.5 Retrofitting Technique using FRP

The retrofitting of structure done by wrapping of FRP has shown that the R.C.C beams change its failure from ductile to brittle. FRP reinforcement is also used for improving the structural behavior. Strengthening concrete beams with FRP reinforcements increased the flexural stiffness and the ultimate load carrying capacity of the strengthened beams compared to the unstrengthened beam (Rizkalla et al.). Non prestressed laminate has been improved the load-deflection behavior of retrofitted beams [3]. The FRP sheet is used for retrofitting the structures. The efficiency of structure has improved by applying the FRP on the tension face. The strengthening of beams using carbon fiber sheets is found to be more effective in improving the flexural strength and ultimate load capacity of beams [17]. FRP are typically organized in a laminate structure, such that each lamina (or flat layer) contains an arrangement of unidirectional fibers or woven fiber fabrics embedded within a thin layer of light polymer matrix material.Various researchers have been studied the effect of FRP Laminates in prestressed and in non prestressed state. The rehabilitation of significantly cracked beams by bonding prestressed CFRP laminates is structurally efficient [4].

## 1.6 Application of FRP

FRP is used in Aerospace, structure rehabilitation, modern bicycle, Automotive Field, Motorcycle. Low Weight to High strength ratio is most attractive properties or main cause of its popularity. Recently its application area has been increasing due to its use in manufacturing of commonly use material such as laptop, Drum, Fishing rod, Paint ball, Tripod etc.

## 1.7 Benefits

FRP composites have many benefits to their selection and use. The selection of the materials depends on the performance and intended use of the product. The composites designer can tailor the performance of the end product with proper selection of materials. A summary of composite material benefits include:

1 Light weight
2 High strength-to-weight ratio
3 Directional strength
4 Corrosion resistance
5 Weather resistance

6 Dimensional stability
7 Radar transparency
8 Non-magnetic
9 High impact strength
10 High dielectric strength (insulator)
11 Low maintenance
12 Long term durability
13 Part consolidation

## 1.8 Objective of thesis

After studying about the properties of different fiber reinforced polymer it has been seen that the carbon fiber reinforced polymer has a improved mechanical properties as compared to other FRP. Although there is a various technique under which CFRP used for retrofitting, described in section 1.6. This study has been carried out to understand the effect of various prestressed level of CFRP on retrofitted beams. The main objective of this thesis is to study the effect of various prestressed level on retrofitted reinforced concrete beams.

## CHAPTER -2

## LITERATURE REVIEW

## 2.1 General

To increase the strength of already built structure or partially damaged structure, the most adoptable technique is retrofitting. Retrofitting of the structure can be done by the various methods. The study of Retrofitting with different methods is elaborated in this chapter. This chapter deals with;

1 Retrofitting of Structural Element by Non Prestressed Fiber Reinforced Polymer

2 Retrofitting of Structural Element by Prestressed Fiber Reinforced Polymer

3 Fiber Reinforced Polymer Debonding Model

4 Effect of Fiber Reinforced Polymer on Columns

## 2.2 RETROFITTING OF STRUCTURAL ELEMENT BY NON PRESTRESSED FIBER REINFORCED POLYMER

**Obaidat et al. (2010)** investigated the behavior of structurally damaged full scale reinforced concrete beams retrofitted with CFRP laminates in shear or in flexure. The main variables in this study are the reinforcement steel ratio and CFRP length. The beam had a rectangular cross section of (1960x300x150mm) .The beam divided into two group (1) RF – it was designed to have insufficient flexural strength to obtained a pure flexural failure.(2) RS – it had a same geometry but were cast with a reduced shear reinforcement ratio and a larger longitudinal reinforcement ratio in order to obtain pure diagonal shear cracks without development of flexural cracks. The schematic diagram of RF and RS is shown below.

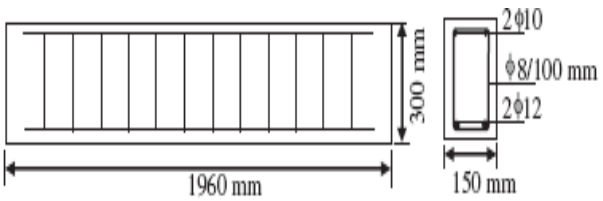


**Fig 2.1 (a) Bems in Group RF**

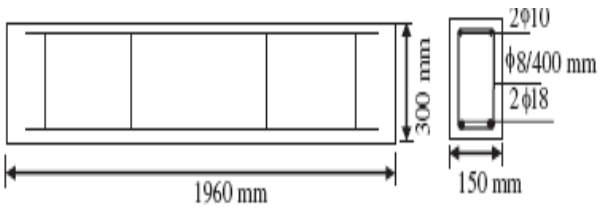


**Fig 2.1 (b) Beams in Group RS**

The beam was tested in four point bending. The span between the support was 1560 mm and the load was applied at point dividing the length into three equal parts. The results shows that the stiffness of the CFRP retrofitted beams is increased compared to that of control beams. The increase in maximum load of the retrofitted specimens reached values of about 23% for retrofitting in shear and between 7% and 33% for retrofitting in flexure. Moreover, retrofitting shifts the mode of failure to be brittle. It also observed that the crack width for the retrofitted beams is decreased compared to the control beams and By increasing the CFRP, plate length in flexural retrofitting can make the CFRP more effective for concrete repair and strengthening .This means that insufficient strengthening lengths do not produce the intended strengthening effect. It also concluded that the main failure mode was plate debonding which reduces the efficiency of retrofitting.

**Swamy et al. (1987)** investigated the effect of glued steel plates on the first cracking load, cracking behavior, deformation, serviceability, and ultimate strength of reinforced concrete beams. Twenty-four beams were tested. Each beam had a rectangular cross section of 155x 255 mm and was 2.5 m long. The beams were reinforced with three 20 mm diameter bars at an effective depth of 220 mm .Three glue thicknesses,1.5 mm,3mm and 6 mm were used. For each glue thickness three plate thicknesses were used: 1.5 mm,3mm and 6 mm, all of constant width of 125 mm. For comparison, several beams were tested with lap plates, double plates, and variable thickness for the glue along the length of the beam. The adhesive thickness varied from 3 mm to 8 mm. The results indicated that the addition of glued steel plates to a reinforced concrete beam can substantially increase the flexural stiffness, reduce cracking and structural deformations at all load levels, and contribute to the ultimate flexural capacity. The net effect of the reduced structural deformations was that the serviceability loads were substantially increased by the stiffening action of the glued plates. Lapped plates, precracking prior to plating variable glue thickness, and the presence of stress concentrations in the adhesive all had no adverse effect on the structural behavior of the plated beams.

**Saadamanesh et al.(1991)** figure out the static strength of reinforced concrete beams strengthened by gluing glass fiber reinforced plastic (GFRP) plates to their tension flanges is experimentally investigated.5 rectangular beams and one T beam were tested to failure under four point bending. The results indicated that the flexural strength of RC beams can be significantly increased by gluing GFRP plates to the tension face. In addition the epoxy bonded

plates improved the cracking behavior of the beams by delaying the formation of visible cracks and reducing crack widths at higher load levels. The design detail of the beams and its schematic diagram shown below.

**Table no 2.1 Design Details of Test Specimens**

| Beam (1) | Compression steel (2) | Tension steel (3) | Number of stirrups (4) |
|---|---|---|---|
| A | 2 No. 4[a] | 3 No. 8[b] | 14 No. 3[c] @ 330 mm (13 in.) |
| B | 2 No. 4 | 2 No. 8 | 34 No. 4 @ 150 mm (6 in.) |
| C | 2 No. 4 | 2 No. 4 | 34 No. 4 @ 150 mm (6 in.) |
| D | 2 No. 4 | 2 No. 8 | 34 No. 4 @ 150 mm (6 in.) |
| E | 2 No. 4 | — | 34 No. 4 @ 150 mm (6 in.) |
| F | 3 No. 4 | 2 No. 8 | 34 No. 4 @ 150 mm (6 in.) |

[a]Nominal diameter of No. 4 bar = 13 mm (½ in.).
[b]Nominal diameter of No. 8 bar = 25 mm (1 in.).
[c]Nominal diameter of No. 3 bar = 9.5 mm (⅜ in.).

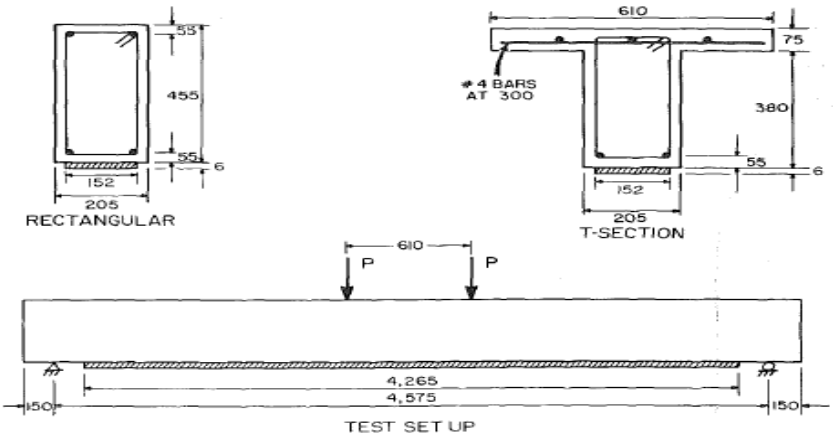


**Fig- 2.2 Cross Sections and Test Setup of Beams**

The results indicated that significant increase in the flexural strength can be achieved by bonding GFRP plates to the tension face of reinforced concrete beams. The gain in the ultimate flexural strength was more significant in beams with lower steel reinforcement ratios. In addition, plating reduced crack size in the beams at all load levels. The successful application of this technique requires a careful preparation of concrete surface and the selection of a tough epoxy. Plating somewhat reduced the ductility of the beams.

**Aiello et al. (2000)** investigated the behavior of FRP reinforced concrete member under service condition. Results of an experimental analysis have been utilized to compare theoretical predictions, furnished by classical approaches (cross section model) and more accurate approaches (block models) in terms of moment curvature and load deflection diagrams. Cross-section models overestimate the FRP reinforced concrete beams' deformability. The block model

adopted in the analysis gives satisfactory results that are in agreement with experimental predictions. However, the procedure of the adopted block model appears onerous from a computational point of view and its use for design practice is difficult in spite of the accuracy of its predictions. The procedure, therefore, can be adopted to obtain numerical data to check the validity of the simplified relationships usually adopted for design practice. For this reason a wider experimental and theoretical investigation is suggested to obtain a meaningful range of data that allows one to both check the validity of the simplified procedures, such as those proposed from the codes, and calibrate the involved parameters. In addition, these data could be useful in defining an analytical relation representing all possible cracking configurations that is able to avoid the use of the two limit curves (I, II). The adopted block model, considering the occurrence of slip, is greatly dependent on the effectiveness of t-*s* laws. However, the definition of a bond-slip relationship of general validity is very difficult, because several parameters are involved. The utilized bond-slip law seems to adequately represent the interaction between concrete and rebars within the tested beams.

**Li et al. (2005)** did experimental and numerical analysis to predict the load carrying capacity of reinforced concrete beams strengthened with carbon fiber reinforced plastics (CFRP) composites. Four point bending test was carried out for rectangular beam in large testing frame of 2000 KN capacity. Size of the beams were L x b x h( 2x.12x.2) clear span 1800 which were designed as under reinforced section. From the test it was concluded that CFRP can effectively increases the initial cracking, ultimate loads, ultimate loads, stiffness, ductility of concrete beams and improve crack patterns. The distance from the end of the fiber to the support point is the main influence on debonding failure. Debonding failure of concrete beams strengthened with CFRP occurs before the normal ultimate load and the high strength property of CFRP cannot be utilized. Debonding failure has greater influence on initial cracking load than on stiffness, ductility and ultimate load of concrete beams and it has a lesser influence on crack pattern. it will greatly influence the performance of strengthened concrete beams and must be considered sufficiently during the design process. Construction procedure and anchorage design procedures may not avoid debonding failure completely.

**Benjeddou et al. (2006)** studied the damaged reinforced concrete beams repaired by external bonding of carbon fiber reinforced polymer composite laminates to the tensile face of the beam. Two sets of beam were studied. Control beams (without CFRP laminates) and repaired beams

with different amounts of CFRP laminates by varying parameters (damage degree, CFRP laminates width, concrete strength class). All beams were tested in four point bending over a span of 1800 mm. The beams dimensions were 2000x120x150 (l x b x h). The span of the beam (1800mm) is limited by the testing machine configuration. After testing these beams were repaired using unidirectional fiber laminates. Five beams were repaired with S1210 having 100 mm width and one beam was repaired with S1250 having 50 mm width. Author concluded that the mechanical performance of the repaired RC beams highly increased by using the CFRP laminates .Therefore this technique is effective to at least restore the mechanical performance of cracked or damaged RC beams. The laminate width affects the failure mode of the repaired beams. This failure mode changes from interfacial debonding to the peeling off when the width increase from 50 mm to 100 mm. Also for a load capacity improvement, reinforcement with a CFRP having about a half width of the beam is satisfactory. Even when the interfacial debonding occurs.

**Rusinowski et al.(2007)** conducted a experimental study in which 7 beams were tested. The specimens were prepared with varying parameters: concrete quality, epoxy adhesive type, adhesive thickness, and amount of tensile reinforcement and CFRP plate type. In order to localize failure a 20-mm-deep notch was made in the centre section of the beams prior to strengthening. Furthermore, a 20-mm-long section on one side of the notch was unbonded to initiate debonding While the other side was prevented from debonding by wrapping with CFRP sheet. All specimens were subjected to 3-point-bending tests, with the load applied in the mid-point. Deflections and support settlements were measured with LVDT. Strain gauges were mounted in three sections on reinforcing steel and CFRP in order to measure strain distribution through height. The description of concrete material used, CFRP used, Adhesive type, Adhesive thickness and Amount of tension reinforcement are given in a table 2.1. The failure mode and their ultimate load are shown in the table 2.3.The crack pattern of beam no 2 is shown in figure 2.10

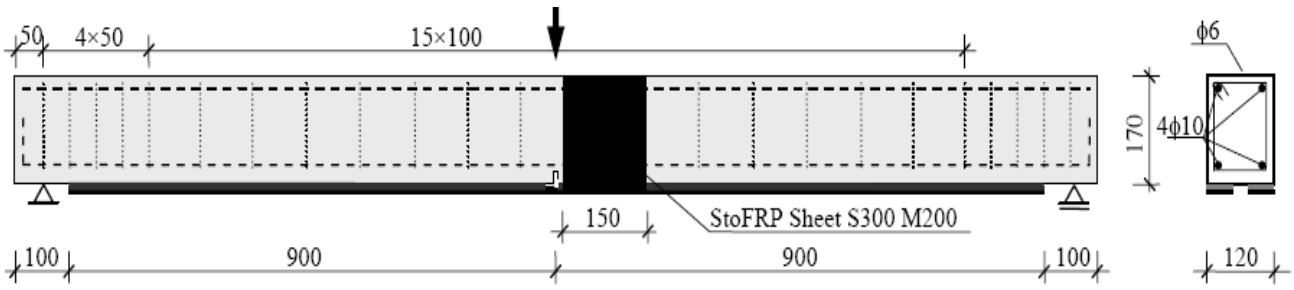


**Fig- 2.3 Geometry and Static System of Strengthened Beam**

**Table-2.2 Test Matrix**

| | Concrete quality | CFRP type | Adhesive type | Adhesive thickness | Tension reinforcement |
|---|---|---|---|---|---|
| Beam 1 (Ref) | High | – | - | - | 2ϕ10 |
| Beam 2 | High | StoFRP Plate E 50 C | StoBPE Lim 567 | 1 mm | 2ϕ10 |
| Beam 3 | High | StoFRP Plate M 50 C | StoBPE Lim 567 | 1 mm | 2ϕ10 |
| Beam 4 | High | StoFRP Plate E 50 C | StoPox Sk 41 | 1 mm | 2ϕ10 |
| Beam 5 | High | StoFRP Plate E 50 C | StoBPE Lim 567 | 1 mm | - |
| Beam 6 | High | StoFRP Plate E 50 C | StoBPE Lim 567 | 2 mm | 2ϕ10 |
| Beam 7 | Low | StoFRP Plate E 50 C | StoBPE Lim 567 | 1 mm | 2ϕ10 |

**Table- 2.3 Failure Modes and Ultimate Load Comparison**

| | Beam 1 | Beam 2 | Beam 3 | Beam 4 | Beam 5 | Beam 6 | Beam 7 |
|---|---|---|---|---|---|---|---|
| Failure mode | Steel yield. | Peeling at flex. crack | Cover separation | Cover separation | Peeling at shear crack | Peeling at flex. crack | Peeling at shear crack |
| Ultimate load [kN] | 29.1 | 72.6 | 68.8 | 69.3 | 30.7 | 69.7 | 58.2 |

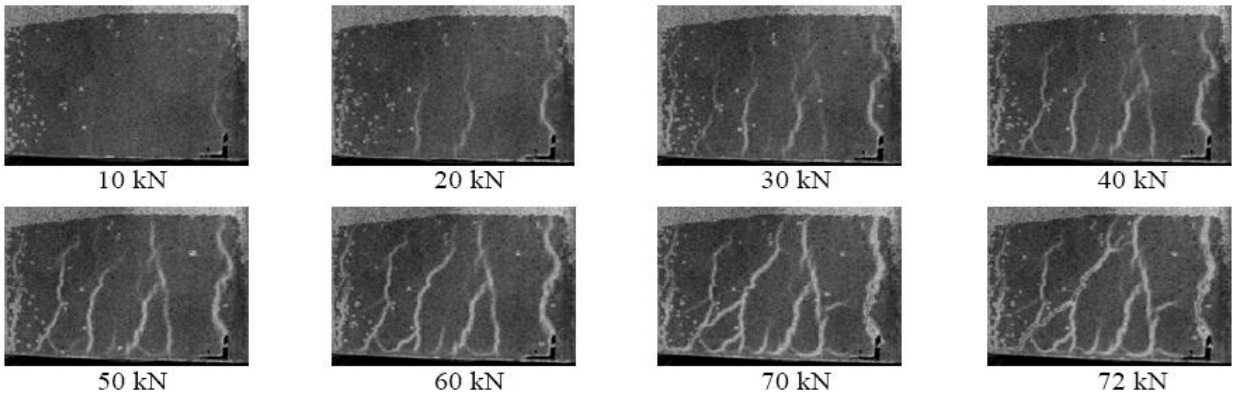


**Fig – 2.4 Crack Distribution in Beam 2 at Different Load Level**

It concluded that the optical equipment was found to be an efficient tool in crack detection and crack width measurement. The debonding occurs due to the initiation of flexural-shear crack in the three-point-bending test. During this experimental program it observed that interlaminar Peeling and concrete cover separation were failure most likely to occur. All strengthened beam failed in different mode followed by initiation of debonding. The concrete cover separation observed in the case of a stiff CFRP plate and finer epoxy adhesive. In case of application of lower quality concrete, debonding of shear crack was combined with concrete cover separation.

## 2.2 RETROFITTING OF STRUCTURAL ELEMENT BY PRESTRESSED FIBER REINFORCED POLYMER

**Zou (2003)** compared the beams prestressed with CFRP tendons and beams prestressed with steel tendons. Under this study he investigated the behavior of both beams for long term deflection and cracking. Six beams with rectangular cross sections 300mmx150mmx6000mm were fabricated and the beams contained only two CFRP tendons and no stirrups nor other longitudinal reinforcement. A particular type of CFRP tendon, tensile strength of 2250 Mpa and elastic modulus of 147000 Mpa was used in four of the beams. Seven wires steel strand tendon, with smooth surface of 8mm in diameter having tensile strength of 1860 Mpa and elastic modulus of 200,000 Mpa was used in other two beams for comparison purpose. Beams were prestressed with the force of 80 kN and 120 kN. Material Prestressing force, and loading condition for both the beams were kept same. Ready mixed concrete of 40 and 80 Mpa concrete strength was used for fabricated beams. Load was applied on all the beams and deflection was checked at 56 days after loading and after 259 days of loading. It was observed that beams casted with CFRP tendons deflected more in initial stage as the beams prestressed with CFRP tendon was less than that of beam prestressed with steel tendon. After 56 days when further loads were applied, beam with steel tendon, and the difference in deflection increased with time .It was concluded that, the instantaneous deflection of beam with CFRP tendon after cracking is more than that of beam with steel tendon and this indicates that sectional stiffness of beams with CFRP tendons was slightly lower than beam with steel tendons due to lower elastic modulus of CFRP. When beams prestressed with CFRP tendons having similar prestressing force but different concrete strength was compared, the beam having higher concrete strength tend to have lower deflection for longer time period . With the increase in concrete strength number of cracks and crack width was also reduced. So it was concluded that that the long-term deflection of beam prestressed by CFRP tendons was comparable to that of identical beams prestressed by steel tendons and beams with the higher concrete strength have lower curvature and lower deflection.

**Mukherjee & Rai (2008)** studied the performance of reinforced concrete beam externally prestressed with carbon fiber reinforced polymers (CFRP) laminates bonded to the RC beam is investigated in terms of the flexural strength, deflection, cracking behavior and failure modes.
The experiment had Several Phase (a) Fresh beam loading(b) Unloading (3) Prestressing (4) Reloading .All the reinforced concrete (RC) beam specimens were loaded under four point bend

test setup. The beams have been loaded with equal force on the two load points until the beams deformed did not take any further load. The loading was discontinued when the load deflection curve was flat and no increase load was observed due to the increase in deflection. It was noticed that the flexural performance of the rehabilitated beams were far superior to that of the fresh RC beams. The beams had higher failure load and lower deflections. They remained in the elastic zone for a much higher applied load. The recovery from the deformation increased with the increased in the prestressing force. As a result ,the area under the load-deflection curve was much higher for the highly prestressed beams. However, the ultimate load and the maximum deflection did not go up significantly with higher level of prestress. It was concluded that for rehabilitation one must decide the amount of CFRP based on the requirement of the ultimate capacities. By prestressing one would be able to achieve a linear load-deflection curve for higher level of loading. Thus results indicate that rehabilitation of significantly cracked beams by bonding CFRP laminates is structurally efficient.

## 2.3 FIBRE REINFORCED POLYMER DEBONDING MODEL

**Mukherjee & Rai (2009)** presented a model which governs the transformed behavior of beams after retrofitting, based on their previous experimental study of prestressed retrofitted beam. For

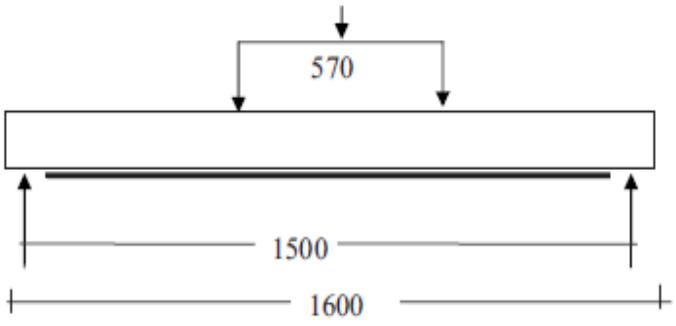


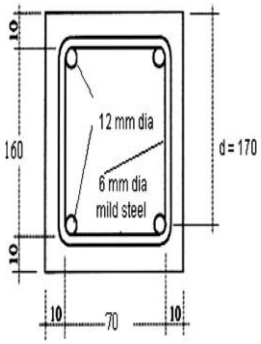


**Fig 2.5(a) Two Point Loading** **Fig 2.5 (b) Cross Section Of Beam**

the load–deflection behavior of the fresh and rehabilated beam has been proposed. The main importance of the model is that it incorporates the effect of confinement of concrete. Experiment had a different stages. first stage of testing called 'fresh beam tests'. All the reinforced concrete (RC) beam specimens have been loaded in a four point bend test setup. This test has been carried out on the RC beams prior to the application of any FRC. The set up ensures pure bending in the central third portion of the beam. The beams have been loaded with equal force on the two load

points until the beams deformed did not take any further load. It may be noted that the beam sections were under-reinforced. Therefore, steel had yielded in all the specimens. The damage in the beams started with bending cracks in the central region of the beam. The beam was rehabilitated. The rehabilitation includes prestressing. The rehabilitated beams have been loaded up to the design load and unloaded The permanent deformation in the beam is measured once

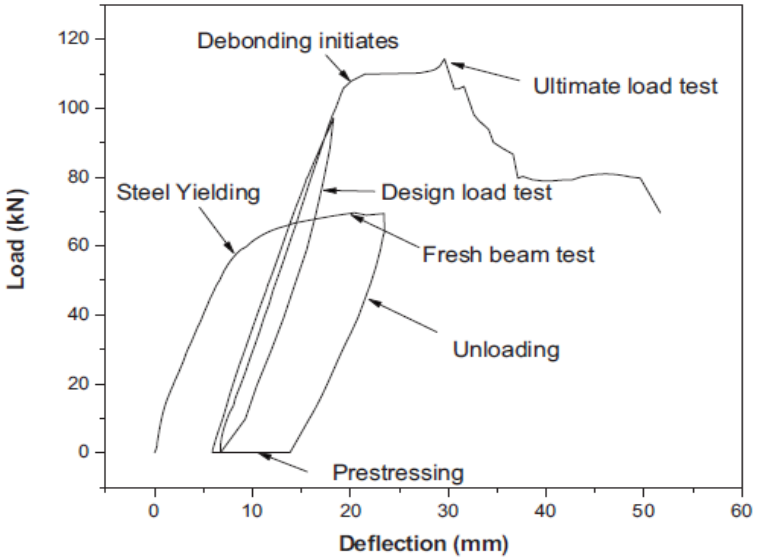


**Fig-2.6 Load Deflection Curve for RC Beams**.

again. The beams have been loaded once again until failure. The prestressing done by specially designed machine. One end of the machine was fixed and other movable. The load deflection graph at all stages of R.C beams is shown in the figure 2.6. The theoretical model has been developed in different scales. The response of a structure under load depends, to a large extent, on the stress–strain relation of the constituent materials. The material scale model has been used on the cross section of the element to obtain a cross-section scale model. This model is in the form of moment–curvature relations for the cross section. Utilizing the cross-section model the element model has been developed to predict the load–deflection relation of the beam. The basic premise of the model is that the constitutive behavior of concrete at low strains before the initiation of damage is governed by its initial modulus ($E_0$). However, the limiting strain $(\varepsilon_{\text{lim}})$ is determined by the level of confinement and the maximum stress is determined by its grade "*f*ck". Therefore, the constitutive model is a function of all these parameters.

$$\sigma_z = E(E_0, f_{\text{ck}}, \varepsilon_{\text{lim}})\varepsilon \qquad (1)$$

$$E = \left(1 - \frac{\varepsilon}{\varepsilon_{\lim}}\right)E_0 + \frac{\varepsilon f_{ck}}{\varepsilon_{\lim}^2}$$

$$\varepsilon_{\lim} = 0.002(1 + 5C_f) \qquad (2)$$

$$C_f = \left(\frac{E_f t_f + E_s t_s}{E_0 r}\right)^{0.5} \qquad (3)$$

$C_f$ = confinement factor,$E_f$ =modulus of elasticity of FRp, $t_f$ =thickness of fiber , $E_s$=modulus of elasticity of steel, $t_s$=thickness of steel, $E_0$=initial modulus of concrete, $r$ =effective radius

The cross section model based on stress strain diagram below.

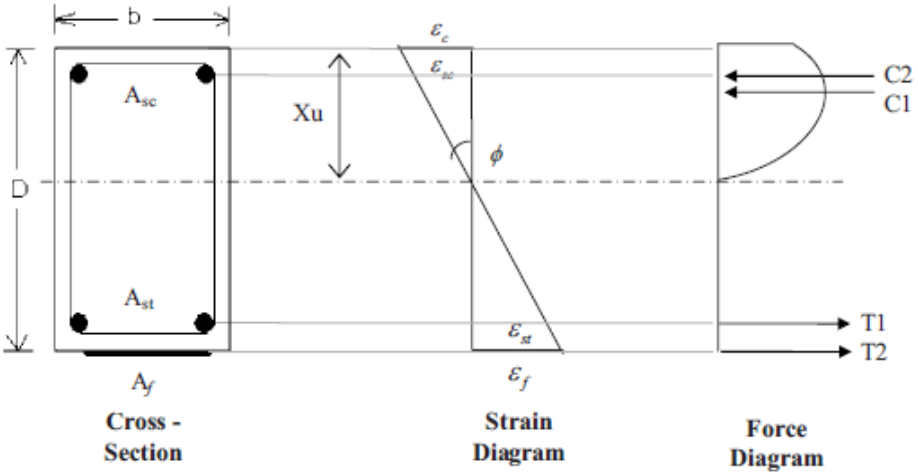


**Fig 2.7 Stress-Strain Distribution Across the Cross Section**

$$\varepsilon_c = \phi X_u$$

$$\varepsilon_{sc} = \phi(X_u - d_c)$$

$$\varepsilon_{st} = \phi(d - X_u)$$

$$\varepsilon_f = \phi(D - X_u) \qquad (4)$$

Where

$\varepsilon_c$= concrete compressive strain at the extreme compression fiber,$\varepsilon_{sc}$=strain in compression steel.$\varepsilon_{st}$=strain in tension steel. $\varepsilon_f$ =strain in plate. ϕ=curvature given to the cross section. $X_u$=depth of neutral axis from compression face. $d_c$=effective cover to the compression steel.

$d$=depth of centroid of tension steel. $b$,$D$=overall width and depth of the cross section , $A_{sc}$ ,$A_{st}$ ,$A_f$ =area of compression steel reinforcement, tensile steel reinforcement, and FRP plate, respectively.

The equilibrium relation for the cross section can be written as:

$$C = \sigma_{sc} A_{sc} + b \int_0^{X_u} \sigma_c dx$$

$$T = \sigma_{st} A_{st} + \sigma_f A_f$$

$$C = T \qquad \textbf{(5)}$$

The equations have been solved numerically for $Xu$ by iterations. The corresponding bending moment for a curvature can thus be calculated.

$$M_c = b \int_0^{X_u} \sigma_c x dx$$

$$M_{sc} = \sigma_{sc} A_{sc} (X_u - d_c) \qquad \textbf{(6)}$$

$$M_{st} = \sigma_{st} A_{st} (d - X_u)$$

$$M_p = \sigma_f A_f (D - X_u) \qquad \textbf{(7)}$$

The bending moment at a section corresponding to the applied curvature is obtained from:

**M = Mc + Msc + Mst + Mp** **(8)**

It concluded that In case of RC beams, failure is characterized by yielding with a large branch of plastic deformation. FRP strengthened beams show marginal change in initial stiffness. A substantial difference in the post yield behavior of the beam is noticed. With the increase in the FRP reinforcement the post yield stiffness increases monotonically. Thus, at a given curvature, the resisting moment of the beam would increase with increase in FRP. However, the maximum curvature also reduces with the increase in FRP. As a result, the beam resists higher bending moments but fails at a lower curvature. Figure 2.8 below shows the load deflection diagram of the fresh beam. It can be seen that the initial stiffness of the experimental curve is higher. However, the beam loses that stiffness at a fairly low level of loading and the two curves come very close. The contribution of concrete in tension is neglected in the theoretical model.

Therefore, the experimental beam shows higher initial stiffness. The curves deviate from linearity through the yielding of steel in tension. Finally, the strain limit of steel is exceeded and that is considered as the failure point. The correlation between the two curves is very good. The post yield hardening behavior of the beam observed in the experiment is not reflected in the numerically obtained plot because the strain hardening is not considered in the theoretical model for steel.

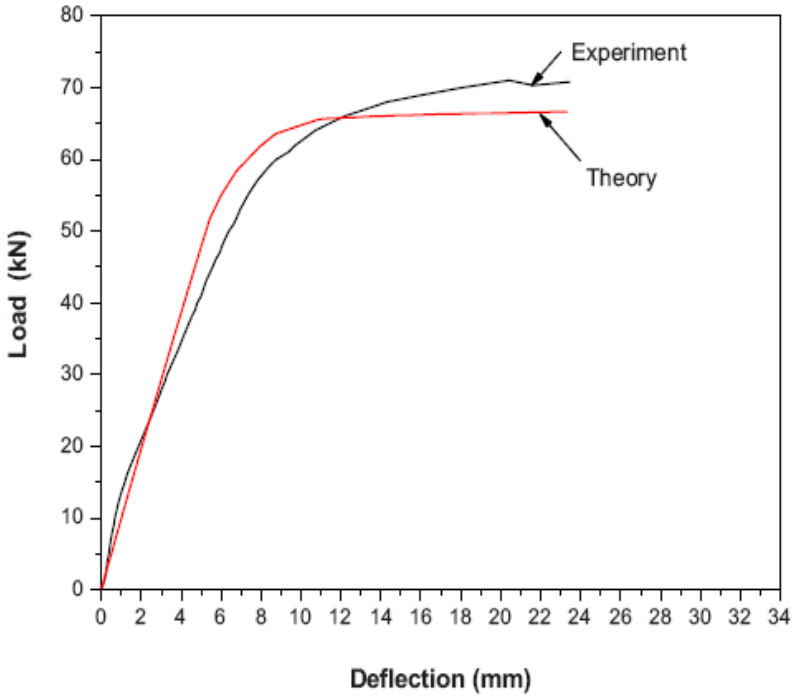


**Fig- 2.8 Theoretical and Experimental Load-Deflection Curve of RC beam**

**Teng et al. (2003)** broadly classified the debonding failure modes. Based on existing studies, a schematic representation of seven typical failure modes observed in test is shown below. These seven failure modes are termed (a) flexural failure by FRP rupture; (b) flexural failure by crushing of compressive concrete; (c) shear failure; (d) concrete cover separation; (e) plate and interfacial debonding ; (f) intermediate flexural crack induced intermediate debonding; and (g) intermediate flexural-shear crack induced interfacial debonding.

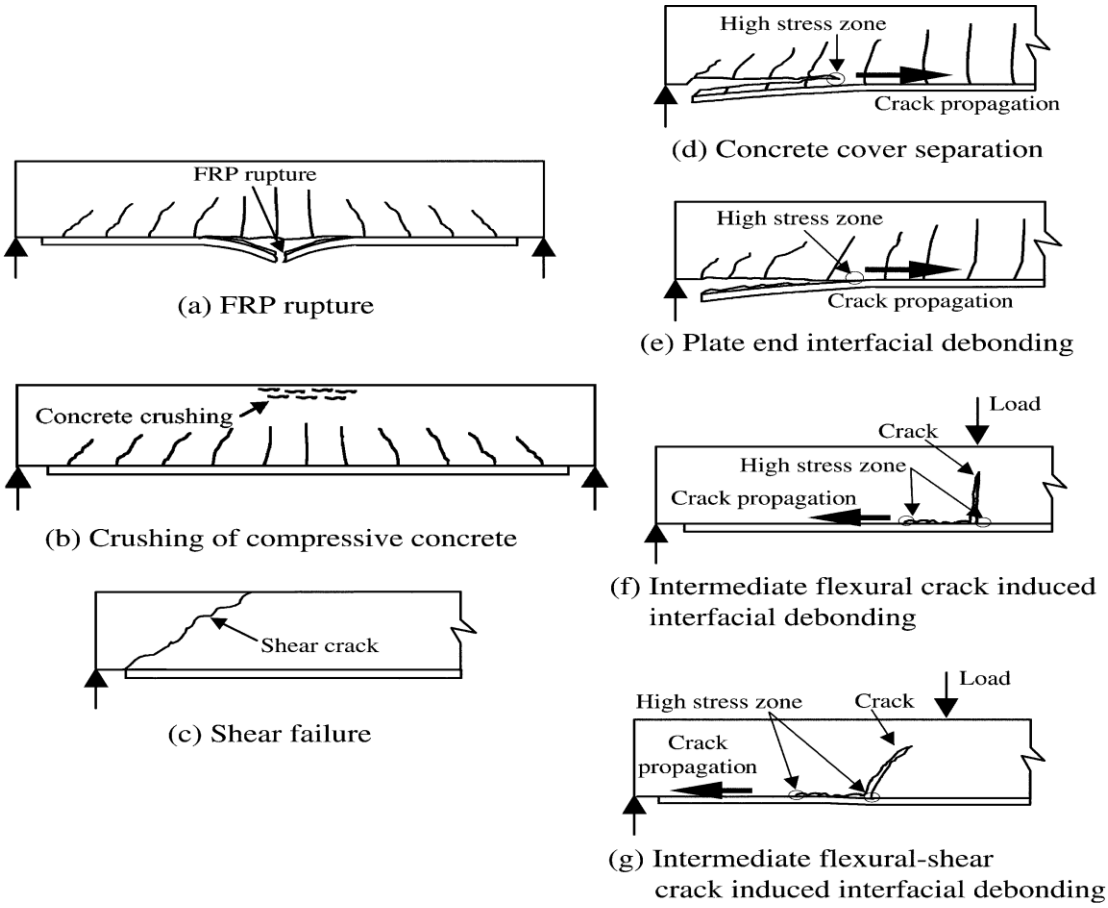


**Fig. 2.9 Failure Modes of RC Beams Flexurally- Strengthened with an FRP Soffit Plate**

The observed modes of debonding in FRP plated beams can be broadly classified into two types: (1) Those associated with high interfacial stresses near the ends of the bonded plate (failure mode (d) and (e)which are collectively referred to the plate end debonding; and (2) Those induced by a flexural or flexural-shear crack away from the plate end (failure modes (d) and (e) which are collectively referred to as intermediate crack-induced debonding (or simply intermediate crack debonding or IC debonding).If no debonding occurs at all the ultimate moment of a section is reached then the concrete failed by crushing. Since the present IC debonding strength model also makes use of a section analysis, the incorporation of the IC

debonding strength model into the existing design equations without consideration of debonding is straight forward. The revised procedure consists of the following three steps:

a. Determination of the ultimate plate stress $\sigma_{dbic}$ for IC debonding according to the following equation:

$$\sigma_{dbic} = 0.48\beta_p\beta_L\sqrt{\frac{E_{frp}\sqrt{f'_c}}{t_{frp}}}$$
$$= 0.45\beta_p\beta_L\sqrt{\frac{E_{frp}\sqrt{f_{cu}}}{t_{frp}}}$$

Where $fcu$ is the concrete cube compressive strength and is taken to be the cylinder compressive strength $fc'$ divided by .8.it should be noted that regardless of the use of any anchorage measures, a sufficient anchorage length should be specified for the FRP plate. it is suggested that the distance from the critical section to the plate end should at least be twice the effective bond length to ensure an anchorage length $La$ of

$$L_a = 2\sqrt{\frac{E_{frp}t_{frp}}{\sqrt{f'_c}}} \approx 2\sqrt{\frac{E_{frp}t_{frp}}{\sqrt{f_{cu}}}}$$

In such cases, $\beta_L = 1$.

b. The reduced tensile strength $f_{frp,r}$ of the FRP plate is worked out as the smaller of the ultimate tensile worked out as the smaller of the ultimate tensile strength $f_{frp,r}$ and $\sigma_{dbic}$ that is $f_{frp,r} = \min(f_{frp,r}, \sigma_{dbic})$

c. The ultimate moment Mu of the critical section under consideration is hten evaluated using existing design with $f_{frp}$ replaced by $f_{frp,r}$

the above three steps procedure is based on the assumption that the same partial safety factor is used for the FRP tensile strength and the plate stress at IC debonding in a limit state design approach, so the reduced tensile strength of the FRP $f_{frp,r}$ is the characteristics strength of the FRP taking into account the effect of IC debonding. However if the partial safety factor for the FRP tensile strength $\gamma frp$ differs from the partial safety factor $\gamma$dbic for the plate stress at IC debonding, then the reduced design value of the FRP tensile strength should be found from

$$f^d_{frp,r} = \min(f^d_{frp}, \sigma^d_{dbic})$$

And the reduced design value $f'_{frp}$ should replace the design value of the FRP tensile strength $f_{frp}^{d}(=f_{frp}^{d}/\gamma_{frp})$ in the design equation. it should be noted that a structural loaded before being strengthened with an externally bonded FRP plate. the effect of this initial loading can be easily included by the use of a modified stress-strain curve for the FRP. This modification is believed to be still valid when the stress of the FRP is limited by IC debonding unless preexistent cracking is so severe that it may significantly affect the behavior of the FRP concrete interface.

**Teng et al (2006)** proposed a simple model to investigate the behavior of FRP–to-concrete interface between two adjacent cracks in flexurally strengthened RC beams. An analytical solution has been presented to predict the entire debonding process of the model under various load combinations. The realistic bi-linear local bond –slip model is employed in the solution. The solution provides closed-form expressions providing a rigorous and complete theoretical basis for understanding the full-range load–displacement behavior of the model .It should be noted that while the emphasis of the paper is on FRP–to-concrete bond interface, the analytical solution is equally applicable to similar interfaces between thin plates of the other materials(e.g. steel and aluminium) and concrete. It may even be applicable to thin plates bonded to members of other materials such as steel and masonry provided a bi-linear local bond-slip model remains a good approximation of local bond behaviour. The general formulation and the solution process can also be extended to interfaces with other local bond slip models.

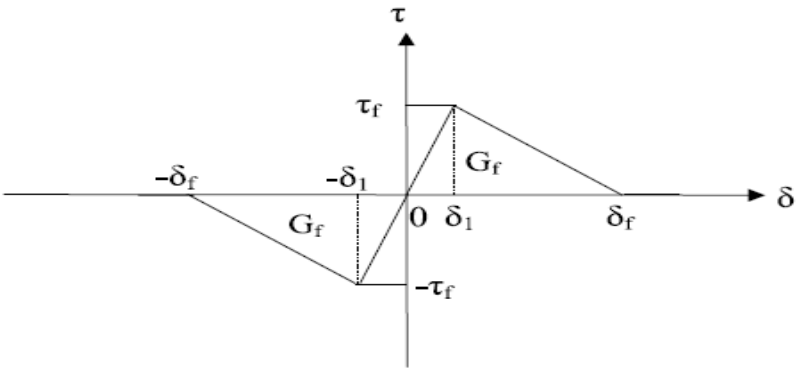


**Fig- 2.10 local bond slip model**

Considering both positive and negative slips, the bond-slip model as shown in above figure can be mathematically described by the following equation:

$$f(\delta) = \begin{cases} \frac{\tau_f}{\delta_1}\delta \quad \text{when } 0 \leqslant |\delta| \leqslant \delta_1 \\ \frac{\tau_f}{\delta_f - \delta_1}(\delta_f - \delta) \quad \text{when } \delta_1 < \delta \leqslant \delta_f \\ \frac{\tau_f}{\delta_f - \delta_1}(-\delta_f - \delta) \quad \text{when } -\delta_f \leqslant \delta < -\delta_1 \\ 0 \quad \text{when } |\delta| > \delta_f \end{cases}$$

It may be noted that before the slip reaches the ultimate value $\pm\delta_f$, the bond-slip relationship is assumed to be fully reversible when local unloading is experienced. Note that this assumption is true when the bond is still elastic but cannot be satisfied in practice if the bond has entered the softening stage. However, in the present case, local unloading after softening only occurs in a very small zone at one end of the bond length Therefore, this assumption can significantly simplify the analysis without significant loss of accuracy. Once the local bond slip model defined then various stages of debonding and interfacial shear stress both analyzed. Various stages of debonding interfacial shear stress can be explained by various schematic diagram shown below.

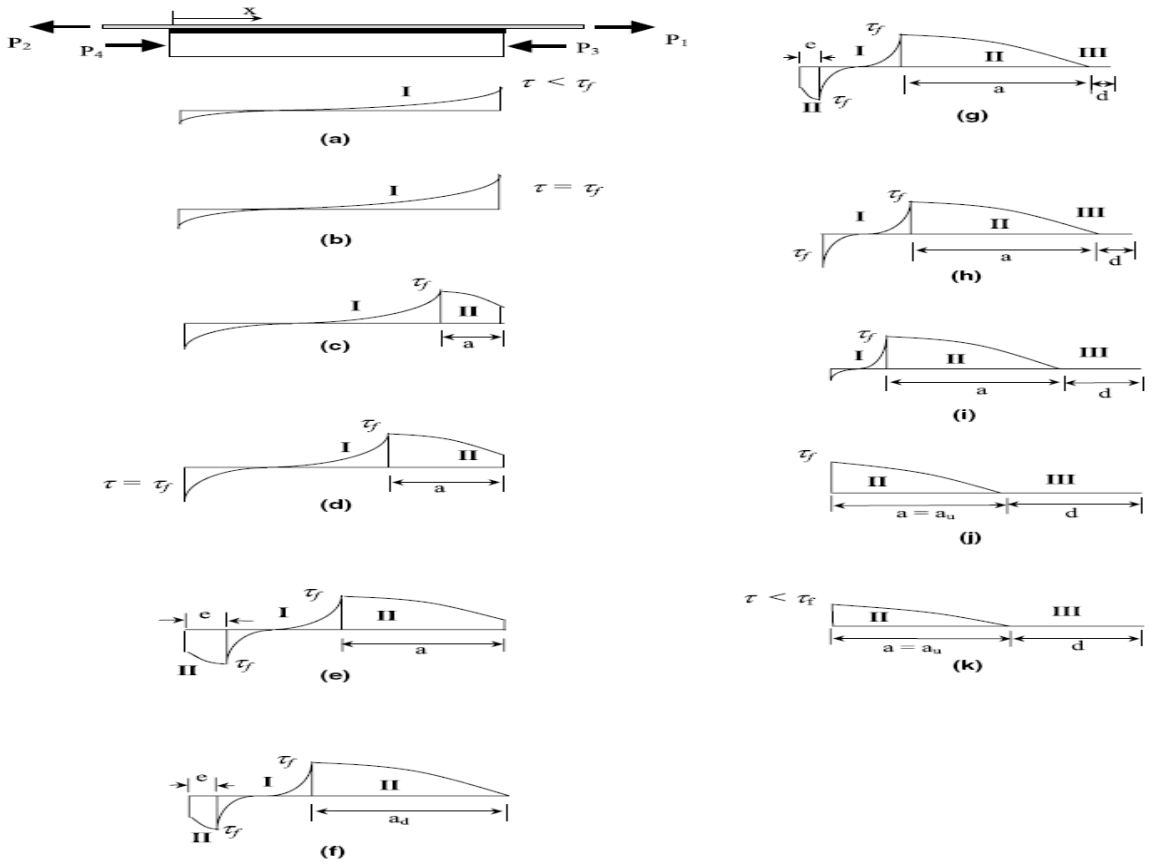


**Fig- 2.11 Interfacial shear stress distributions at various stages**

**(a)** Elastic stress state **(b)** Initiation of softening at x = L **(c)** Propagation of softening zone **(d)** Initiation of softening at x = 0 **(e)** Propagation of both softening zones **(f)** Initiation of debonding

at x = L **(g)** Propagation of debonding **(h)** Disappearance of softening at x = 0 **(i)** Propagation of debonding **(j)** Peak shear stress at x = 0 **(k)** Linear unloading

It concluded that analytical solution has identified five possible failure processes for FRP-to-concrete interfaces. The bond length and the load parameter ß are the key factors governing these failure processes. Each of these failure processes has been examined in detail through a numerical example. The ultimate load increases with the load parameter ß and becomes infinite for any bond length if ß is equal to 1 (i.e. when the FRP plate is subject to equal but opposite tensile forces at both ends). Similar to the simple pull tests of FRP-to-concrete bonded joints, an effective bond length also exists for FRP-to-concrete joints with the FRP plate tensioned at both ends. The numerical examples show that the effective bond length is about 1.2 times the characteristic softening length $a_u$ which depends on many geometrical, material and loading parameters. The ultimate load of the bonded joint increases with the bond length before the effective length is reached and remains constant thereafter.

**Golder et al 2005** investigated the bond strength and critical bond length for the FRP with concrete prism . The test result for single shear tests conducted on concrete prisms bonded with variety of FRP and metallic plates to evaluate the bond strength and the critical bond length required to sustain the maximum stress on bond for a given plate- concrete interface. The elastic modulus and ultimate tensile strength of the plates of different material vary between 32-300 GPa and 196-2800 MPa respectively. Various numerical equations were derived to evaluate the bond strength and critical bond length. The strain variation along the bonded joint at various loads levels, and the shear stress as a function of load level was determined for all the tests. The crack propagation was monitored visually. The following relation were developed to evaluate the various parameter.

**Axial strain and shear stress distribution**

$$\tau_{i-j} = [t_p E_p (g_i - g_j)/\Delta l_{i-j}]$$

$t_p$ –plate thickness $g_i$ and $g_j$ measured strain magnitudes at two consecutive gauge location *I* and *j*.Ep elastic modulas of plate.$\Delta l_{i-j}$ .Table 2.4 showing the test result of all the specimen

**Table 2.4 specimen studied during experimental study**

| Test series | Specimen reference no. | Bond length, $L_b$ (mm) | Width of plate, $b_p$ (mm) | Thickness of plate, $t_p$ (mm) | Measured strain ($10^{-6}$) | Initial cracking load (kN) | Measured ultimate failure load, $P_u$ (kN) | Axial tensile capacity of plate, $f_pA_p$ (kN) | Theoretical load, $P_b$, Eq. (11a) and (11b) (kN) | Failure mode |
|---|---|---|---|---|---|---|---|---|---|---|
| GFRP-32.7 | G32.7-100 | 100 | 30 | 4.00 | 4080 | 7.87 | 12.50 | 46.00 | 10.79 | CF |
| | G32.7-150 | 150 | 30 | 4.00 | 4770 | 12.12 | 17.74 | 46.00 | 16.18 | CF |
| | G32.7-175 | 175 | 30 | 4.00 | 5050 | 5.12 | 20.50 | 46.00 | 18.87 | CF |
| | G32.7-200 | 200 | 30 | 4.00 | 4340 | 18.00 | 20.60 | 46.00 | 20.24 | CF |
| | G32.7-250 | 250 | 30 | 4.00 | 7135 | 18.10 | 20.40 | 46.00 | 20.24 | CF |
| | G32.7-300 | 300 | 30 | 4.00 | 6535 | 14.98 | 20.30 | 46.00 | 20.24 | CF |
| Aluminium-74.8 | Al74.8-150 | 150 | 30 | 6.00 | 1370 | 12.00 | 19.44 | 35.28 | 16.14 | CF |
| | A74.8-200 | 200 | 30 | 6.00 | 1025 | 10.12 | 25.14 | 35.28 | 22.59 | CF |
| | Al74.8-250 | 250 | 30 | 6.00 | 1120 | 17.50 | 24.90 | 35.28 | 26.89 | CF |
| | Al74.8-280 | 280 | 30 | 6.00 | 1730 | 10.00 | 26.02 | 35.28 | 27.67 | CF |
| | A74.8-300 | 300 | 30 | 6.00 | * | * | 25.40 | 35.28 | 27.67 | CF |
| Steel-208 | S208-50 | 50 | 50 | 1.72 | * | * | 11.30 | 48.60 | 9.83 | CF |
| | S208-75 | 75 | 50 | 1.72 | * | * | 16.25 | 48.60 | 17.52 | CF |
| | S208-100 | 100 | 50 | 1.72 | 730 | 12.78 | 22.12 | 48.60 | 21.90 | CF |
| | S208-125 | 125 | 50 | 1.72 | * | * | 21.25 | 48.60 | 25.63 | CF |
| | S208-150 | 150 | 50 | 1.72 | 1580 | 15.10 | 22.80 | 48.60 | 25.63 | CF |
| | S208-200 | 200 | 50 | 1.72 | 1475 | 17.54 | 23.50 | 48.60 | 25.63 | CF |
| | S208-255 | 255 | 50 | 1.72 | 1350 | 17.50 | 22.90 | 48.60 | 25.63 | CF |
| CFRP-C165 | C165-100 | 100 | 50 | 1.20 | 1530 | 14.40 | 18.25 | 168.00 | 21.25 | CF |
| | C165-130 | 130 | 50 | 1.20 | * | * | 24.50 | 168.00 | 27.25 | CF |
| | C165-150 | 150 | 50 | 1.20 | 3425 | 15.08 | 28.44 | 168.00 | 31.87 | CF |
| | C165-175 | 175 | 50 | 1.20 | 2900 | 20.32 | 32.00 | 168.00 | 34.23 | CF |
| | C165-200 | 200 | 50 | 1.20 | 3160 | 27.46 | 34.22 | 168.00 | 34.23 | CF |
| | C165-250 | 250 | 50 | 1.20 | 2825 | 20.36 | 33.14 | 168.00 | 34.23 | CF |
| | C165-300 | 300 | 50 | 1.20 | 3150 | 26.00 | 34.24 | 168.00 | 34.23 | CF |
| CFRP-C210 | C210-150 | 150 | 50 | 1.20 | * | * | 30.40 | 144.00 | 26.93 | C F&FF |
| | C210-180 | 180 | 50 | 1.20 | 2265 | 27.80 | 34.00 | 144.00 | 32.30 | C F&FF |
| | C210-190 | 190 | 50 | 1.20 | * | * | 36.00 | 144.00 | 35.90 | C F&FF |
| | C210-200 | 200 | 50 | 1.20 | 2040 | 30.12 | 36.02 | 144.00 | 36.03 | C F&FF |
| | C210-230 | 230 | 50 | 1.20 | 1750 | 32.00 | 37.02 | 144.00 | 36.03 | C F&FF |
| | C210-255 | 255 | 50 | 1.20 | 2250 | 30.10 | 36.80 | 144.00 | 36.03 | C F&FF |
| CFRP-C300 | C300-160 | 160 | 50 | 1.20 | 1000 | 10.00 | 38.02 | 78.00 | 34.31 | C F&FF |
| | C300-180 | 180 | 50 | 1.20 | 920 | 25.24 | 41.15 | 78.00 | 38.60 | C F&FF |
| | C300-200 | 200 | 50 | 1.20 | 1920 | 24.80 | 46.35 | 78.00 | 40.96 | C F&FF |
| | C300-250 | 250 | 50 | 1.20 | 1880 | 20.16 | 45.50 | 78.00 | 40.96 | C F&FF |
| | C300-300 | 300 | 50 | 1.20 | 1345 | 17.54 | 45.95 | 78.00 | 40.96 | C F&FF |

*Note*: The size (width and thickness) of the specimens in all the six series is 100 mm × 100 mm. CF, concrete fracture; CF&FF, concrete fracture and fibre fracture/fibre inter-laminar failure; *, data not recorded/not available; $f_c$, cylindrical compressive strength of concrete; $E_c$, Young's modulus of concrete; $f_p$, tensile strength of plate; $E_p$, Young's modulus of plate; $f_b = 0.53(f_c)^{0.5}$ (ACI 318-89) [31].

**Expression for critical length $L_{b,crit}/t_p$**

The major parameter that affect the magnitude of critical length are modulus of elasticity $E_p$ of plate, thickness of plate $t_p$, splitting tensile strength of concrete $f_b$ and tensile strength of plate $f_p$.

$L_{b,crit}/t_p = .0089x^3 - 0.439x^2 + 7.8645x$ Where $x$ is a non-dimensional parameter, and is given by

$$x = (E_p^{.25} f_p^{.125} / t_p^{.25} f_b^{.25})$$

**Expression for $P_b$**

$$P_b = \frac{K_{crit}\beta_p\left(\frac{L_b}{t_p}\right)}{\left(\frac{L_{b,crit}}{t_p}\right)} f_b t_p b_p, \quad \text{if } L_b/t_p < L_{b,crit}/t_p.$$

$$K_{crit}\beta_p f_b t_p b_p, \quad \text{if } L_b/t_p \geq L_{b,crit}/t_p.$$

$P_b$ is always greater than A$pf$p where $f$p =ultimate strength in case of linear elastic plates like FRP and yield strength in case of metallic plates.

It was concluded that the direct single shear tests have shown that the debonding in reinforced concrete prisms, retrofitted with bonded steel, aluminium or FRP plate is always caused due to the initiation of the cracks in the vicinity of the most stressed end. The tensile strength of the plate has an effect on both the ultimate strength and critical bond length as determined from the test. These critical parameters are found to depend on elastic modulus, tensile strength, width, and thickness, of the plate, as well as tensile strength of concrete and width factor. The design guidelines developed in this study are capable of predicting the ultimate bond strength of beams bonded with metallic and non metallic plate with very good accuracy, and the model is validated with large number of test result

## 2.4 EFFECT OF FIBER REINFORCED POLYMER ON COLUMNS

**Mukherjee. A. et al.(2004)** studied on the mechanical response of concrete columns confined with fiber-reinforced polymer composites (FRP). Practical columns often deviate from axisymmetric conditions due to noncircular cross section, geometric imperfections, and loading eccentricities. This paper discusses these complicating effects on the mechanical behavior of columns confined with FRP. Experiments have been carried out to examine the effects of geometric and loading imperfections on columns of various shapes. A model originally developed for axisymmetric situations has been extended to include the complicating effects. An analytical study for the corner radius that avoids concentration of stress is carried out. The theoretical models have been verified with the present and published experimental results. Axial stress-strain curves for bare circular (CB1) wrapped circular (C1) square (S4) and rectangular (R1) specimens under concentric loading condition are plotted in Fig 2.18. It was observed that all the specimens confined by glass-fiber wraps showed a considerable increase in ultimate strength over the unconfined specimen (CB1).The detail of specimen with different cross sections and loading conditions are shown below.

**Table – 2.5 Specimens With Different Cross Sections And Loading Conditions**

| Description | Specimen number | Dimension | Details of FRP | Loading condition |
|---|---|---|---|---|
| Circular | C1 | 100 diameter×750 long | GF | C |
| | C2 | 100 diameter×750 long | GF | Ec−20 mm |
| | C3 | 100 diameter×750 long | GF+CLW | Ec−20 mm |
| | C4 | 100 diameter×750 long | GF+CLW | C |
| Square | S1 | 100×100×1,000 long (CR=5 mm) | GF | C |
| | S2 | 100×100×1,000 long (CR=5 mm) | GF | Ec−20 mm |
| | S3 | 100×100×1,000 long (CR=7.5 mm) | GF+CFP | Ec−20 mm |
| | S4 | 100×100×1,000 long (CR=11.3 mm) | GF | C |
| Rectangular | R1 | 85×180×850 long (CR=7.5 mm) | GF | C |
| | R2 | 85×180×850 long (CR=7.5 mm) | GF | Ec−20 mm |
| | R3 | 85×180×850 long (CR=7.5 mm) | GF+CFP1 | C |
| | R4 | 85×180×850 long (CR=7.5 mm) | GF+CFP1 | Ec−20 mm |
| Rectangular with ties | RH1 | 85×180×850 long (CR=7.5 mm) | GF+CFP2 | Ec−20 mm |
| | RH2 | 85×180×850 long (CR=7.5 mm) | GF+CFP2 | C |
| | RH3 | 85×180×850 long (CR=7.5 mm) | GF+CFP2 | Ec−10 mm |

Note: FRP=fiber-reinforced polymer; GF=0.4-mm-thick glass-fiber wrap; CLW=longitudinal carbon-fiber wrapping; CFP1=40-mm-wide longitudinal carbon-fiber strips on each long face; CFP2=2×20-mm-wide longitudinal carbon-fiber strips on each long face; RH=rectangular column with 10-mm-diameter holes at 150 mm c/c filled with glass FRP ties along the length; C=concentric loading; Ec=eccentric loading; CR=corner radius.

The stress-strain relationships of the specimens with the same level of confinement were similar. However, the ultimate strain of specimens of a noncircular section was much less than the ultimate strain of the circular sections. As a result, the ultimate strength of the noncircular specimens was less than that of the circular columns.

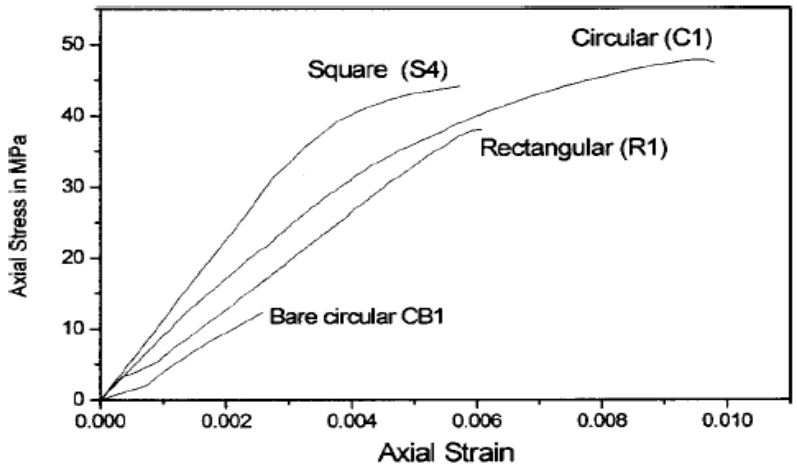


**Fig 2.12- Axial Stress versus Axial Strain for Different Cross Section under Concentric Loading**

The effective confinement is defined in terms of confinement factor $C_f$.

$$C_f = \left( \frac{E_f 2nt/d}{E_0} \right)^{0.67}$$

$E_0$=intial modulus of concrete core; $E_f$= Elastic modulas of Wrap; $n$=No of wrap

$t$= thickness of fiber wrap; $d$= diameter of concrete core

It may be noted that the contribution of the adhesive in the stiffness of the warp is negligible. Therefore, in the present work the elastic modulus of the bare fiber and the effective thickness of the wrap have been used. For the theoretical analysis the model of complicating effects and

effect of imperfection was studied. The former case concerned with the noncircular shapes and the later case concerned with the effect of geometric imperfection and loading imperfection. The following relation were drawn for understanding these parameter. For noncircular cross sections, the diameter *d* is replaced by an equivalent diameter $d_{eq}$.. The diameter of the equivalent circle depends on the geometrical dimensions of the section and the radius at the corners. A power-law expression is developed including these two parameters.

$$C_f = \left(\frac{2E_f nt}{E_0 d_{eq}}\right)^{0.67}$$

the efficacy of the wrap varies exponentially with the corner radius. Therefore, an exponential relation is used between the corner radius and the confinement factor.

$$d_{eq} = b + \frac{444}{e^{0.4\rho}}$$

where *b* shorter cross-sectional dimension in mm; and ρ=corner radius in mm. The numeric coefficients have been found out through regression of the present and previous experimental data. The geometric imperfection has a relation of

$$C_r = 1 - \frac{(\lambda)^{1.05}}{128}$$

where λ slenderness ratio, given as *L*/*r* min ; *L*=effective length; and *r*min=least radius of gyration of the column. The factor $C_r$ is used as a modification factor on the predicted ultimate strength of a standard column:

$$\sigma z(\text{ ult/long}) = \sigma z\ (\text{ult/standard}) X C_r$$

The effect of eccentric loading on the mechanical behavior of a carbon FRP confined columns is hitherto unpublished. In the present paper, a few conclusions have been arrived at based on the experiments carried out so far. . The result indicates that the strength of the column under eccentric loading is lower than that under concentric loading. The ratio of strength of the eccentric columns to the concentric columns is proportional to the ratio of the eccentricity of loading (*e*) and the least radius of gyration (*r*min). It was concluded from the study that the FRP confinement is most effective for columns of circular cross section. For noncircular cross section, although the stiffness of the columns remains close to that of circular ones, the ultimate strain of the column decreases. As a result, the ultimate strength also decreases. The failure of concentrically loaded noncircular columns takes place at the corners. The maintenance of a

minimum corner radius is of great importance for noncircular columns. A modification of the confinement factor has been proposed to model noncircular columns. The factor determines the diameter of an equivalent circular column. The effect of geometric imperfection is included as a modification factor based on the slenderness ratio of the columns. Due to the loading imperfections, it is found that the ultimate load reduces in the same proportion as the ratio of the eccentricity and the radius of gyration .The predicted results are in close agreement with the present experimental results and those of other investigators.

**Hacha et al (2011)** concluded the size effect of concrete specimen confined with the newly developed SFRP sheets and compare the results with conventionally used CFRP sheets. The experimental program included 9 small scale cylinders (150x300) which consisted of three unwrapped, three CFRP and three SFRP wrapped cylinders. The large-scale specimens consisted of three columns (300x1200 mm) composed of unwrapped, CFRP and SFRP wrapped columns. The main objective of this paper is to study the size effect of the CFRP and SFRP confined concrete on the behaviour of the ultimate compressive strength, axial strain, hoop strain and ductility. The main results are summarized in Table given below. Group A results are presented as the average value of the three specimens and the vertical line shown at the tip of the bar graphs represents the standard deviation (+1 $\sigma$ ).

**Table – 2.6 Summary of Group A and Group B compression test results.**

| $G^A$ | C | ID | COMPRESSIVE STRENGTH (MPa) | | AXIAL STRAIN (με) | | HOOP STRAIN (με) | | DUCTILITY (MN-mm/mm) | |
|---|---|---|---|---|---|---|---|---|---|---|
| | | | Max[c]. | Avg. [Std. Dev.][d] | Max. | Avg. [Std. Dev] | Max. | Avg. [Std. Dev] | Total | Average |
| A | I | CT-1 | 44 | 42 | 3000 | 2200 | 380 | 380 | 1500 | 1000 |
| | | CT-2 | 40 | | 1200 | | 360 | | 516 | |
| | | CT-3 | 42 | | 2300 | | 400 | | 1100 | |
| | II | CFRP-1 | 54 | 58 | 7700 | 4300 | 15000 | 9800 | 4700 | 4100 |
| | | CFRP-2 | 58 | | 2800 | | 7500 | | 3500 | |
| | | CFRP-3 | 61 | | 2500 | | 7100 | | 4200 | |
| | III | SFRP-1 | 100 | 97 | 16000 | 16600 | 15000 | 14300 | 21300 | 31400 |
| | | SFRP-2 | 95 | | NA* | | 16000 | | 51400 | |
| | | SFRP-3 | 95 | | 17000 | | 12000 | | 21500 | |
| B | I | CT | 37 | - | 640 | - | 390 | - | 870 | - |
| | II | CFRP | 51 | - | 2000 | - | 550 | - | 5700 | - |
| | II | SFRP | 63 | - | 5000 | - | 4900 | - | 1700 | - |

$G^A$ = Group, C = Category, Max[c]. = Maximum, Avg. [Std. Dev.][d] = Average [Standard Deviation], and NA*= Not Applicable [Strain Gauge Damage].

It is always expected that greater confinement pressure is provided by smaller specimens. In order to understand above statement, the confinement pressure exerted by the wrapped FRP sheets for the circular columns provided by the ACI Committee 440.2R is presented as follows:

$$f_l = \frac{2E_{ju} n t_j \varepsilon_{fe}}{D}$$

$f_l$ =is the confinement pressure

$E_{ju}$ is the modulus of elasticity of the FRP sheets

$n$ is the number of layer

$t_j$ is the thickness of FRP sheets

$\varepsilon_{fe}$ is the effective strain in the FRP sheet

$D$ is the diameter of the circular confined specimen

Equation above implies that the confinement pressure is a function of the size of the cross-section *D*. The equation also implies that the confinement pressure is inversely proportional to the cross-sectional dimension. Based on the confinement pressure illustrated in Figure 2.19, it can be clearly seen that as the size of the column increases, the maximum confinement pressure provided by a given thickness of the FRP wrap reduces.

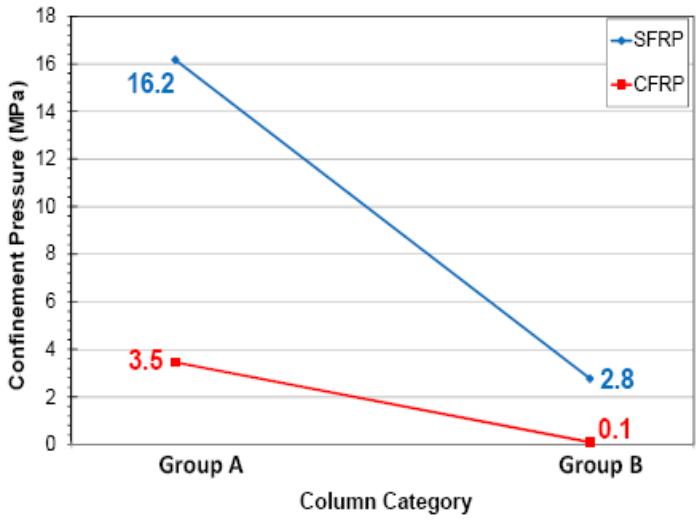


**Fig-2.13 Confinement Pressure of Group I and Group II columns**

From the compression tests of the CFRP and SFRP wrapped specimens, it concluded that by Increasing the size of the specimens significantly affects the ultimate axial strength, axial strain, and hoop strain of CFRP and SFRP wrapped columns, when compared to small-scale specimens. The ductility parameter of the unwrapped and the CFRP wrapped specimens are insignificantly

altered by the size effect. However, increasing the size of the SFRP wrapped column significantly affected the ductility parameter when compared to the small-scale SFRP wrapped cylinders. For a given thickness of the CFRP and the SFRP wrap, increasing the size of the specimen decreases the confinement pressure imposed on the specimen.

**Stratford et al (2011)** studied the mechanics of FRP confined concrete, with a particular emphasis on the influence of the unconfined concrete compressive strength on confinement effectiveness and hoop strain efficiency. An experimental programme was undertaken to study the compressive strength and stress-strain behavior of unconfined and FRP confined concrete cylinders of different concrete strength. Through the use of high-resolution digital image correlation to measure both axial and hoop strains, the observations yield insights into the mechanics of FRP confinement of concretes of similar composition but with varying unconfined concrete compressive strength. The experimental program consisted of uniaxial compressive tests on 30 plain or FRP wrapped concrete cylinders, as outlined in Table below. Test parameters included: (1) the presence of FRP confinement and (2) the unconfined concrete compressive strength.

**Table –2.7 Detail of the Experiment Program and Selected test results.**

| GROUP[a] | FRP (Y/N) | AVE. UNCONF. COMP. STRENGTH (MPa) | FAILURE MODE[b] | FAILURE STRESS (MPa) | | AXIAL STRAIN AT PEAK STRESS (%) | | HOOP STRAIN AT PEAK STRESS (%) | |
|---|---|---|---|---|---|---|---|---|---|
| | | | | Test | $M \pm \sigma^c$ | Test | $M \pm \sigma^c$ | Test | $M \pm \sigma^c$ |
| U-25 | N | 25 | Shear | 22.6 | 25.1 ± 5.8 | 0.41 | 0.28 ± 0.11 | 0.92 | 0.55 ± 0.34 |
| | | | Cone | 31.7 | | 0.26 | | 0.25 | |
| | | | Shear | 20.9 | | 0.18 | | 0.48 | |
| W-25 | Y | | FRP rupture | 55.8 | 58.9 ± 3.6 | 1.12 | 1.24 ± 0.11 | 0.80 | 0.86 ± 0.06 |
| | | | FRP rupture | 62.8 | | 1.27 | | 0.90 | |
| | | | FRP rupture | 58.1 | | 1.33 | | 0.89 | |
| U-30 | N | 30 | Cone | 30.1 | 30.0 ± 1.4 | 0.26 | 0.26 ± 0.02 | 0.32 | 0.29 ± 0.06 |
| | | | Cone | 31.3 | | 0.25 | | 0.22 | |
| | | | Cone | 28.5 | | 0.28 | | 0.33 | |
| W-30 | Y | | FRP rupture | 63.6 | 60.8 ± 2.5 | 0.91 | 0.85 ± 0.06 | 1.05 | 1.11 ± 0.07 |
| | | | FRP rupture | 60.1 | | 0.84 | | 1.19 | |
| | | | FRP rupture | 58.7 | | 0.79 | | 1.09 | |
| U-36 | N | 36 | Cone | 34.9 | 35.7 ± 2.2 | 0.27 | 0.23 ± 0.04 | 0.32 | 0.25 ± 0.09 |
| | | | Cone | 38.2 | | 0.24 | | 0.15 | |
| | | | Cone | 34.0 | | 0.19 | | 0.29 | |
| W-36 | Y | | FRP rupture | 64.8 | 69.3 ± 4.0 | 0.86 | 0.89 ± 0.06 | 0.72 | 0.78 ± 0.08 |
| | | | FRP rupture | 72.3 | | 0.85 | | 0.75 | |
| | | | FRP rupture | 70.8 | | 0.96 | | 0.87 | |
| U-58 | N | 58 | Cone | 55.4 | 57.5 ± 3.1 | 0.27 | 0.28 ± 0.02 | 0.24 | 0.23 ± 0.06 |
| | | | Cone | 61.1 | | 0.28 | | 0.17 | |
| | | | Cone | 56.0 | | 0.30 | | 0.28 | |
| W-58 | Y | | FRP rupture | 77.8 | 79.6 ± 1.7 | 0.47 | 0.58 ± 0.22 | 0.48 | 0.83 ± 0.31 |
| | | | FRP rupture | 79.9 | | 0.84 | | 0.93 | |
| | | | FRP rupture | 81.1 | | 0.44 | | 1.08 | |
| U-66 | N | 66 | Cone | 69.6 | 66.0 ± 5.2 | 0.12 | 0.21 ± 0.13 | 0.20 | 0.20 ± 0.00 |
| | | | Shear | -- | | -- | | -- | |
| | | | Cone | 62.3 | | 0.30 | | 0.20 | |
| W-66 | Y | | FRP rupture | 80.9 | 84.6 ± 5.3 | 0.58 | 0.51 ± 0.07 | 0.62 | 0.56 ± 0.05 |
| | | | FRP rupture | 90.7 | | 0.51 | | 0.54 | |
| | | | FRP rupture | 82.3 | | 0.45 | | 0.53 | |

[a] All tests were performed in triplicate.
[b] FRP rupture = tensile rupture of the FRP wrap in the hoop direction outside the overlapping region.
[c] Note that $\sigma$ is determined for a sample size of $n = 3$, rather than $n - 1 = 2$

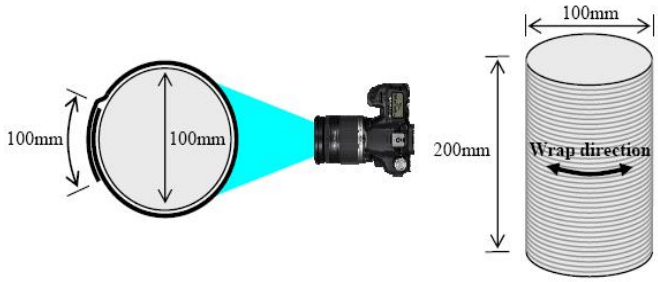


**Fig -2.14 Detail of specimens, FRP wrap Configuration, and Camera Position**

The major conclusion found from the experimental study is that the large increases in compressive strength can be achieved for both low and high strength concretes by applying FRP hoop wraps. the hoop strain at failure (i.e. the tensile rupture strain in the FRP wrap) is highly variable but remains essentially constant with increasing unconfined concrete strength. This suggests that the level of confinement provided by the FRP at the ultimate state is not affected by the unconfined concrete strength, as should be expected. The level of axial strain enhancement due to FRP wrapping appears to decrease considerably as a function of unconfined concrete compressive strength, however the precise reasons for this are not clear. The level of confinement provided by the FRP at the ultimate state does not appear to be greatly affected by the unconfined concrete compressive strength.

# CHAPTER-3

# EXPERIMENTAL PROGRAM

## 3.1 Introduction

The center of attention of this experimental program is to study the behavior of retrofitted R.C.C beams under different prestressing level of carbon fiber reinforced polymer. Mode of failure, crack pattern, type of failure of CFRP also observed in this experimental program. The load versus deflection of controlled specimen and retrofitted with different amount of prestressing forces also pragmatic.

## 3.2 Material

### 3.2.1 Cement

Portland pozzolana cement was used for casting the beams. The PPC cement was in fine powder state and free from lumps and moisture. The various physical properties of cement tested as per IS 1489-1991 part (1) are listed Table 3.1.

**Table 3.1 Properties of Cement**

| Sr No | Characteristics | Test values | Values specified by IS 1489-1991 |
|---|---|---|---|
| 1 | Standard Consistency | 32 | ---------- |
| 2 | Initial Setting time (min) | 122 | 30 min (minimum) |
| 3 | Final Setting Time (min) | 285 | 600 min (maximum) |
| Compressive strength | | | |
| 1 | 7 days | 26 $N/mm^2$ | 22 $N/mm^2$ (minimum) |
| 2 | 28 days | 32 $N/mm^2$ | 33$N/mm^2$ (maximum) |

### 3.2.2 Fine Aggregate

The fine aggregate for the experiment was locally arranged and conformed to Indian standard specification IS 383-1970.The sand was sieved through 4.75mm sieve to remove the particle greater than 4.75mm IS sieve and then was washed to remove the dust. The physical properties of sand are shown in a table 3.2

**Table 3.2 Physical Properties of Fine Aggregate**

| Sr. No | Characteristics | Value |
|---|---|---|
| 1 | Type | Natural sand |
| 2 | Specific Gravity | 2.52 |
| 3 | Water absorption | 1.03 % |
| 4 | Bulk density | 1.4 |
| 5 | Grading Zone | III |
| 6 | Fineness Modulus | 2.34 |

### 3.2.3 Coarse Aggregate

Locally available crushed coarse aggregates of 20 mm were procured for the experimental study .Before using it for casting of beams, tests were performed. The results are shown in a table 3.3.The sieve analysis of 20 mm size aggregate is shown in a Table 3.4

**Table 3.3 Physical Properties of Coarse Aggregate**

| Sr No | Characteristics | Value |
|---|---|---|
| 1 | Type | Crushed |
| 2 | Specific Gravity | 2.60 |
| 3 | Moisture content (%) | .32 |
| 4 | Water absorption(%) | 1.92 |
| 5 | Fineness modulus | 6.87 |
| 6 | Maximum size | 20 mm |

**Table 3.4 Sieve Analysis of 20 mm Coarse Aggregate**

| S.No. | Sieve No. | Mass retained (gm) | Percentage mass retained | Cumulative percentage retained, C | Percentage Passing, (100 – C) |
|---|---|---|---|---|---|
| 1 | 80 mm | 0 | 0 | 0 | 100 |
| 2 | 40 mm | 0 | 0 | 0 | 100 |
| 3 | 20 mm | 0 | 0 | 0 | 100 |
| 4 | 10 mm | 2648 | 88.26 | 88.26 | 11.74 |
| 5 | 4.75 mm | 324 | 10.80 | 99.06 | .94 |
| 6 | pan | 28 | .94 | Sum=187.32 | |

Total weight = 3Kg

FM of 20 mm Coarse aggregate = (187.32+500)/100 = 6.87

### 3.2.4 Water

Water used for mixing and curing shall be clean and free from injurious amounts of oils, acids, alkalis, salts, sugar, organic materials or other substances that may be deleterious to concrete or steel. Clean and fresh water was used for casting and curing the specimens in the experimental study.

### 3.2.5 Reinforcement

12 mm and 8mm Diameter bars were used for preparing the R.C.C beams. HYSD steel of Grade Fe 500 was used. 8mm diameter bar were used as a compression reinforcement as well as for shear stirrups and 12 mm diameter bars were used as a tension reinforcement.

### 3.2.6 Carbon Fiber Reinforced Polymer

300 x .117 mm ( B x H ) Size of CFRP sheet used for the Retrofitting. The Physical properties of CFRP shown in Table 3.5

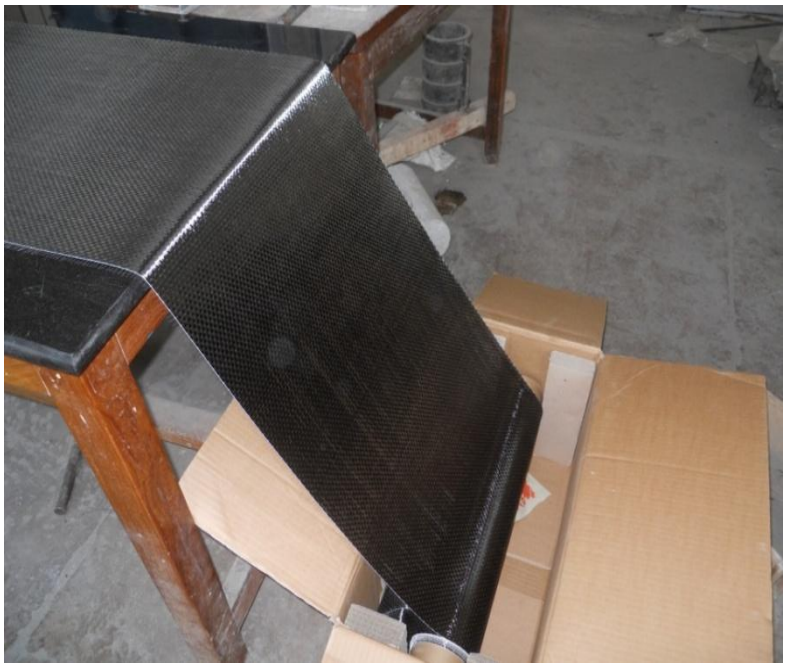

**Fig- 3.1 CFRP Sheet**

**Table -3.5 Physical Properties of CFRP**

| Sr. No | Physical Properties | Value |
|---|---|---|
| 1 | Tensile Strength | 3800 $N/mm^2$ |
| 2 | Modulus of Elasticity | 240 x $10^3$ $N/mm^2$ |
| 3 | Density | 1.7 $g/cm^3$ |
| 4 | Thickness | .117 mm |

### 3.2.7 Saturant

The MBrace composite strengthening system is a family of lightweight FRP materials, externally bonded to the surface of structures .For this experimental study MBrace saturant was used . It was a blue pigmented epoxy resin for saturation of MBrace fiber sheet to form in-situ FRP composite. It was prepared by mixing base saturant and hardner in ratio 100:40. The Properties of the saturant provided by the manufacturer is shown in table 3.6.

**Table -3.6 Properties of MBrace Saturant Provided by Manufacturer**

| | |
|---|---|
| Aspect | Translucent blue liquid |
| Volume Solid | 100% |
| Mix Density | 1.13±0.03 |
| Mixing Ratio (Weight) | 100 to 40 |
| Mixed Viscosity (cps at 25º C | 4000± 500 |
| Pot Life (minutes) | 25 min at 25º C |
| Setting Time | < 3hrs at 25º C |
| Full Cure | 7 days at 18º C |
| Compressive strength | >40 Mpa at 1 day<br>>60 Mpa at 1 days |
| Tensile Strength | >17 Mpa |
| Flexural Strength | >35 Mpa |
| Density | 0.8 to 1 kg/$m^3$ |

### 3.2.8 Roller

The special type of roller was provided by the manufacturer for the proper adhesion of fiber reinforced polymer to concrete surface. Precautions were taken during the application of saturant on the surface of concrete. Pressure was applied by hand on the roller during rolling, for the proper adhesion of FRP to the surface of concrete.

**Fig-3.2 Roller For Spreading the Saturant of CFRP**

### 3.2.9 Linear Variable Differential Transducer

LVDT was used in this experimental study to measure the deflection of Specimens. LVDT transducer has a deflections range of 50mm and has the least count of 0.01mm. The deflection were measured at two places , at the center and l/4 of the span.


**Fig-3.3 Liner Variable Differential Transducer**

### 3.2.10 Prestressing Machine

Specially designed machine was used for prestressing the fiber. It consist of two parts

1 Fixed end

2 Movable end

Fixed end plate consist of heavy metal plate, which is fixed at one end by using mechanical anchor bolt. A CFRP sheet is sandwiched between the concrete surface and fixed end plate. The hydraulic jack is fix by the nut bolt system at the movable end. The force is apply by the jack on the movable arm, With the movement of movable arm the force is transfer to the fiber. The force is apply on the fiber sheet till the required elongation obtained.

**Fig 3.4 (a) Movable Arm**

**Fig 3.4 (b) Fixed End Plate**

### 3.2.11 Hydraulic Jack

Hydraulic jack of 500 kN capacity was used for applying the prestressing to fiber sheet. it was fixed at the vertical plate for applying force at the movable arm. These kinds of jacks operate both vertically and horizontally for use in a variety of lifting, pushing and spreading application. In this experimental program hydraulic jack was used in horizontal direction.

### 3.2.12 Anchor Bolt

Anchor Bolts of 12 mm diameter were used for fasten the fixed end plate and movable end plate of prestressing machine

## 3.3 Design of Beam

Reinforced concrete beams designed as under reinforced section. The sectional dimensions (4.1 x .6 x .3m) were fixed in such a way that during loading it failed under flexural state. 12 mm diameter bars were used in tension face of beam and 8 mm diameter bars were used in compression face. The design details are given in a figure no 3.5.

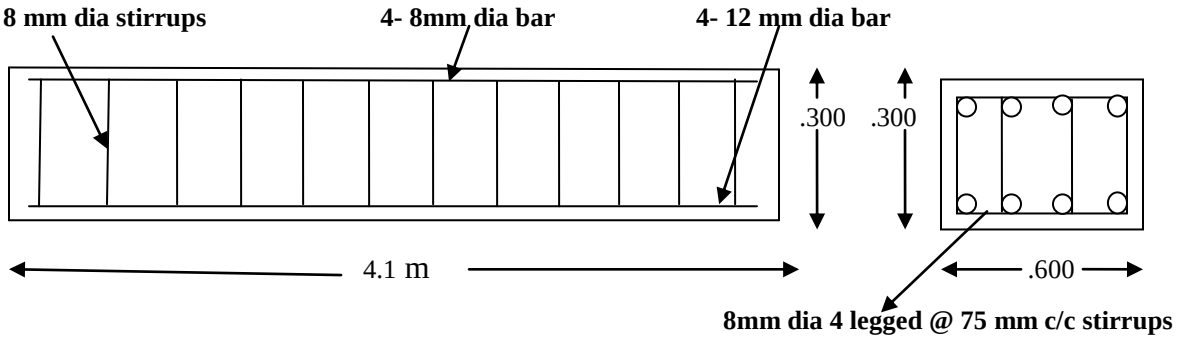


**Fig-3.5 Dimensions of R.C.C Beams**

## 3.4 Concrete Mix

M20 grade of concrete prepared for casting the Reinforced concrete beams. All significant tests regarding materials of mix have done prior to casting. Concrete mixes prepared as per guidelines given in Indian standard code

## 3.5 Casting of Beam

Metal plate shuttering was prepared before casting of R.C.C beam. Cutting and binding of reinforcement has been done as per design and drawing detail. A steel cage prepared manually, before putting it into the shuttering the cover blocks of 25 mm were placed on all sides of shuttering. The fresh mixed concrete was poured and simultaneously proper vibration has been done so that voids come out and densest state of concrete could be achieved.

## 3.6 Experimental Outline

6 beams of sizes (4.1x.6x.3m) were tested under two point loading set up. Two controlled beams were damaged fully to obtain the load versus deflection curve. The details of specimens are given in a Table 3.7.

**Table-3.7 Experimental Outline**

| Sr No | Identity of specimen | Prestressing force (%)based on ultimate tensile strength of CFRP | Quantity of specimen |
|---|---|---|---|
| 1 | Control Beam<br>FDB 01<br>FDB 02 | --- | 2 |
| 2 | Stressed beam [1] | 0 % | 1 |
| 3 | RDB 60 | 60% | 2 |
| 4 | RDB 80 | 80% | 2 |

## 3.7 Detail of Experimental Work

6 beams of sizes (4.1x.6x.3m) were tested under two point loading set up. All beams were loaded individually until individual beams reached at their required stressed level. Load was controlled by the Data Acquisition servo Control System. The load versus time graph and load versus deflection graph were shown by the software. To measure the deflection, Linear Variable Data

Transducer (LVDT) was used at the center and l/4 of the span. LVDT was placed at the top side of reinforced concrete beams.. Two point loading system illustrated in figure 3.6.

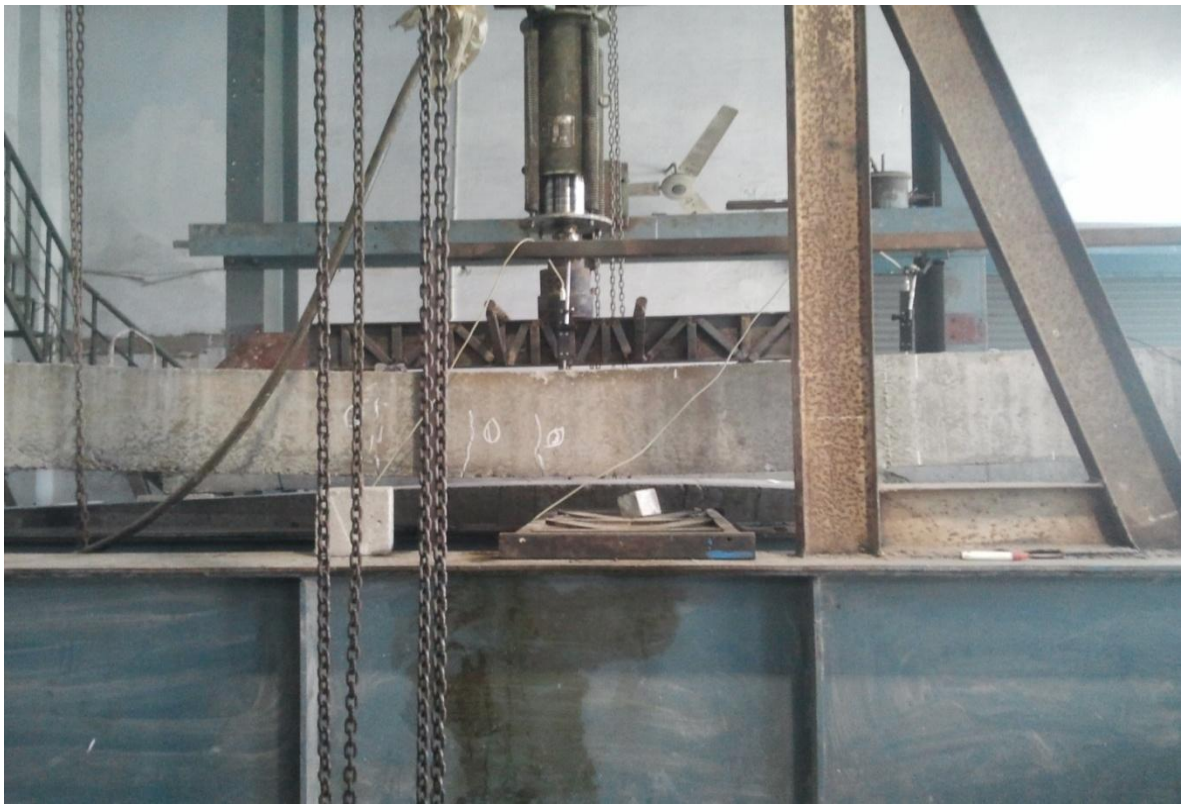

**Fig-3.6 Two Point Loading System**

### 3.7.1 Process of Retrofitting

The retrofitting of initially stressed beams were done as discussed below

- Grinding of tension face
- Installation of CFRP sheet at one end and prestressing machine at other end
- Prestressing of CFRP by hydraulic jack.

#### 3.7.1.1 Grinding

For grinding, the beams were put upside down as shown in fig 3.7. Grinder was applied at the tension face to expose the aggregate surface. Grinder has a diamond plate to grind the concrete surface up to required thickness. Holes were drilled in the beam for fixing the prestressing machine. Uniform and leveled surface of exposed aggregate always have a benefit of developing a efficient bond between the concrete surface and CFRP.

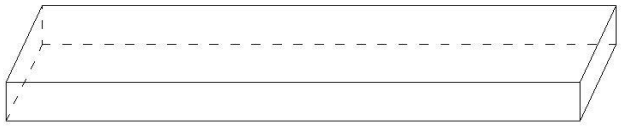

Beam Laid With Compression face upward

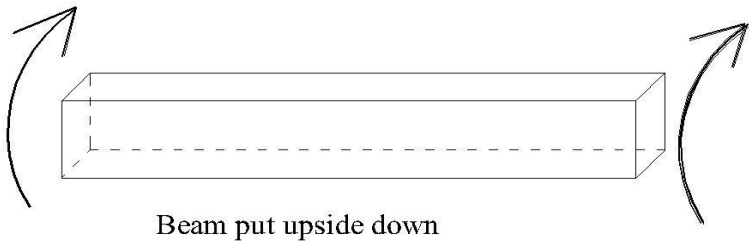

Beam put upside down

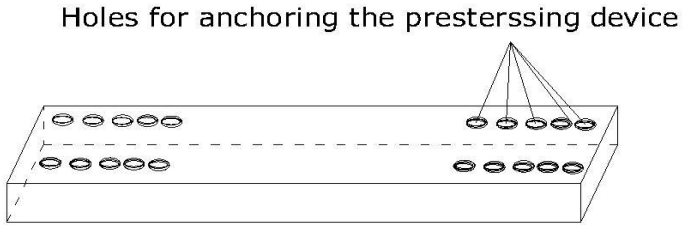


Tension Face Upside

STAGE -1

**Fig-3.7 Beam put Upside Down (stage-1)**

### 3.7.1.2 Installation of CFRP Sheet at One End and Prestressing Machine at Other End

CFRP has cut as per the dimensions required for the specimens. Carbon fiber has a very high tensile strength. To take the ultimate advantage of this mechanical propertie, CFRP has been applied at the tension side of reinforced concrete beam. MBrace saturant was applied on the prepared surface of concrete beam and CFRP sheet was adhered at the fixed end of concrete beam. After the application of rolling, CFRP sheet was sandwiched in between the fixed end plate and beam with the help of Fasteners, which is shown in fig 3.9. The Schematic diagram of prestressing machine is shown in fig 3.8

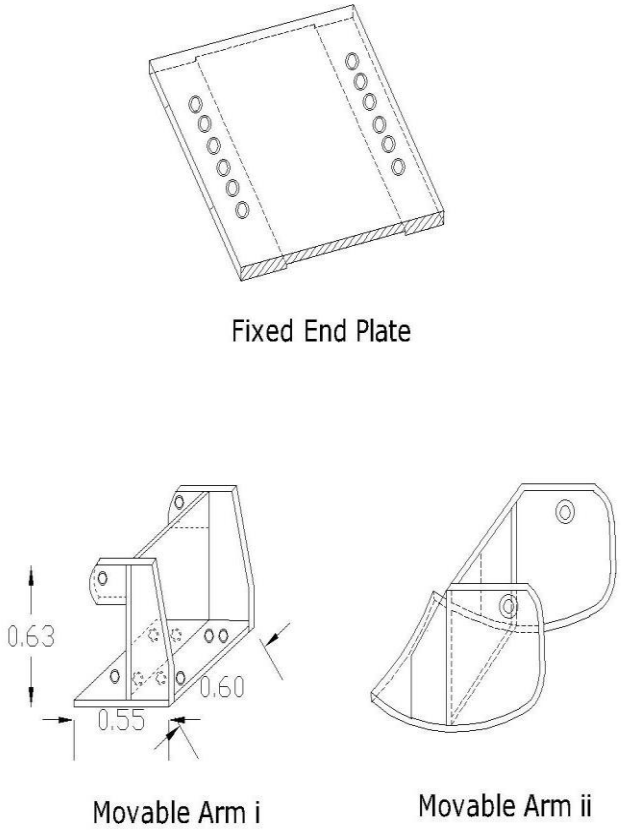


**Fig- 3.8 Prestressing Machine**

Movable end was fixed with the help of fastner. Saturent was applied at the curved surface of movable component of prestressing machine. Another additional plate was fixed at the movable end to supressed the CFRP.The additional plate was applied for the uniform prestressing. Movable end with additional plate is showing in a figure 3.10

**Fig-3.9 Fixing of Fixed End Plate at One End With the Help of Fastner**

**Fig-3.10 Movable End With Additional Plate to Suppressed the CFRP**

The CFRP was attached firmly at the movable end.The instalation of CFRP at fixed end and movable end is shown in Fig 3.11(a) and 3.11 (b). The effective length of CFRP was properly stretched. Manifest streaching image of the CFRP during pasting is shown in fig 3.12.

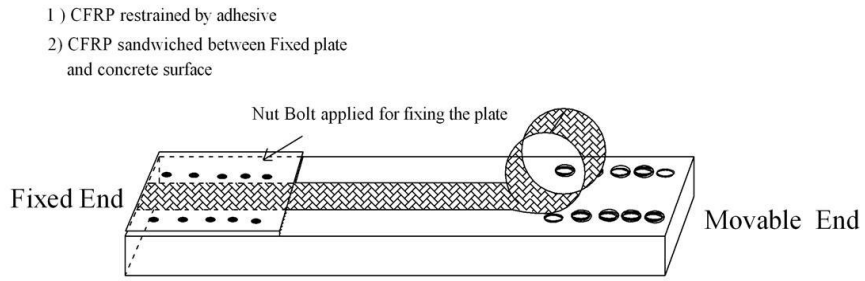


Tension Face Upside and Compression Face Downside

STAGE- 2

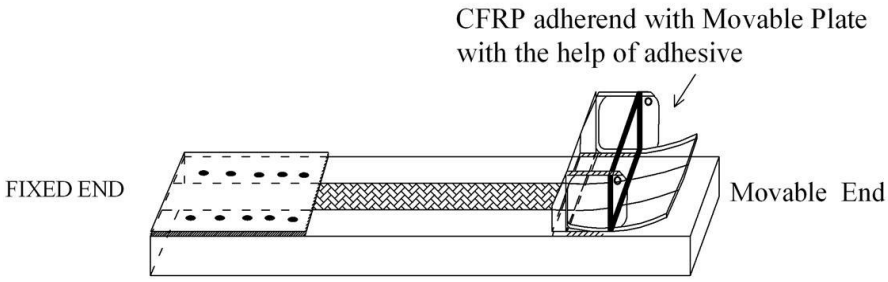


Tension Face Upside and Compression Face Downside

STAGE- 3

**Fig -3.11 (a) Installation of CFRP at Fixed End (stage-2)**

**(b) Installation of CFRP at Movable End (stage-3)**

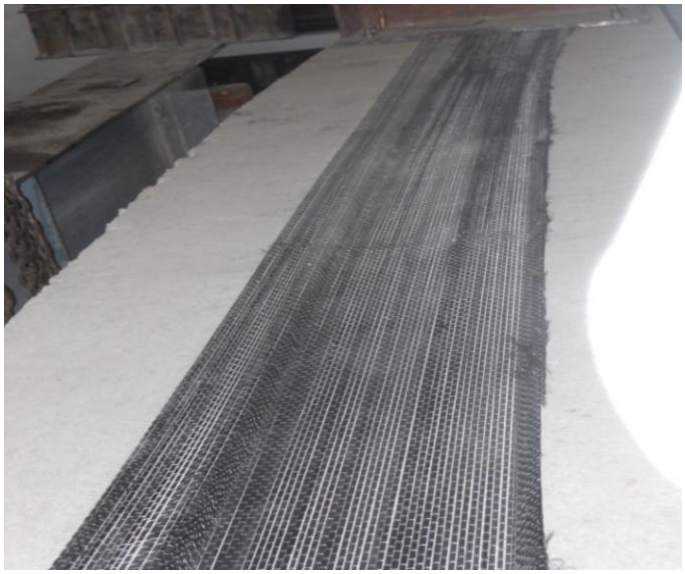

**Fig-3.12 Proper Streaching of Efective Length of CFRP**

### 3.7.1.3 Prestressing of CFRP by Hydraulic Jack.

After the proper fixing of CFRP at both ends it was left for curing for one day. CFRP was glued with soffit of concrete specimen and movable end only.Rest part of fiber was not pasted, which is called effective length of CFRP. The effective length of CFRP shown in the figure 3.12. After the 24 hours of curing the CFRP was ready for the prestressing. Hydrulic jack was fitted at the fixed portion of movable end plate to prestressed the CFRP. During prestressing, the bonding of CFRP with movable curved plate makes possible to transfer the load on CFRP. The reqired force calculated in terms of elongation. Linear variable data transducer (LVDT) was used for the measurment of elongation. Figures 3.13 and 3.14 are showing the prestressing of CFRP. The prestressing has stopped, after getting the required elongation. The saturent was applied on the remaining effective length of CFRP. The proper application of rolling is very important to adherend the CFRP with the concrete surface.Rolling was done untill the epoxy came out from the fiber.The fixing of adittional plate at movable end and prestressing by jack is shown in fig 3.15. It was left for curing for 48 hours and after that jack was released. The U-strip of CFRP was applied at both ends of beam so that there is no pelling off of CFRP from the end. The beam was ready for testing after the proper adhesion of CFRP. Load deflection curves are plotted and compared with the controlled specimen

**Fig -3.13 Prestressing of CFRP**

**Fig-3.14 LVDT Used for Measuring the Elongation of CFRP**

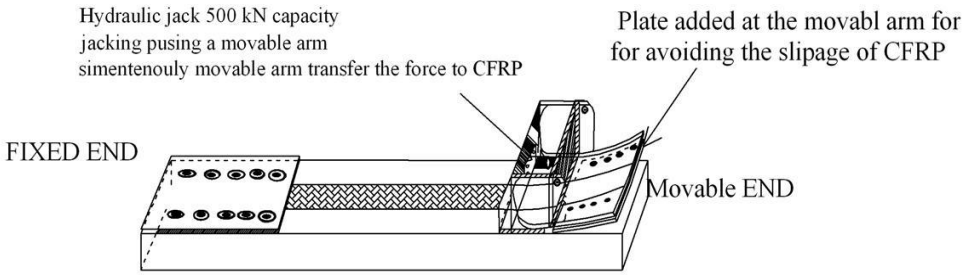


STAGE- 4

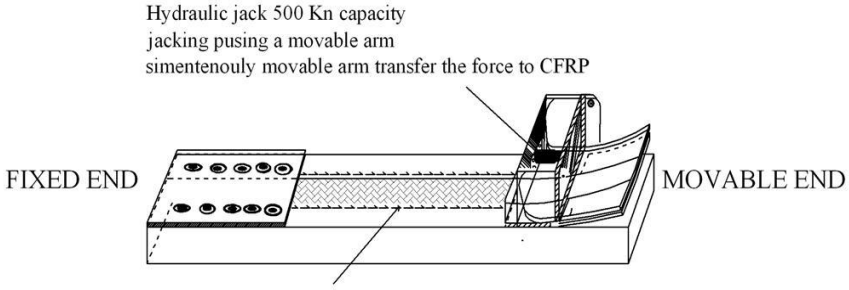


STAGE-5

**Fig-3.15 (a) Additional Plate Applied at Movable end (Stage-4)**

**(b) Prestressing applied by Hydraulic Jack (Stage-5)**

# CHAPTER- 4

# RESULT AND DISCUSSION

## 4.1 Introduction

The results of experimental work are discussed in this section.The load deflection graph of both controlled and retrofitted specimens were obtained. From both controlled specimens graph, one average graph is prepared. The results of intially stressed retrofitted with single non prestressed layer of CFRP sheet [1] has been used for more deterministic conclusion. The other 4 beams were stimulated for fully damage state.Load deflection curves of Retrofitted beams are also compared with the controlled specimens.

### 4.2 Results of Control Beam

#### 4.2.1 Introduction

All beams were tested under the two point loading arrangment.Load deflection values of specimen, first crack load, cracking pattern, yielding of steel were observed during testing.

#### 4.2.2 Control beam (FDB 01)

For establising the foundation of the experiment, first of all (FDB 01) tested under the two point loading system.As the loading was increased beam started to deflect downward side.At a load value of 55 kN first crack was observed, it occur in between the left point load and center of the beam .with the further increase of load, crack started to widenend and propagate towards upside. It was observed that hair line cracks propagate easily in the tension zone and gets more time to propagate in the compression zone, as it is well known that concrete is strong in compression.The second crack was propagate under the left point load when the load reached at 67 kN. At the 73 kN load third crack was observed near the centre and inside the right loaded point. From the graph it is observed that yielding of steel has started at 78 kN. The major cracking has been observed at 88 kN.Beam has stopped taking load at 94.9 kN. During testing it was observed that the crack was straight at the pure bending region.Cracks were widened apart in the bending region. The crack pattern shown in the figure 4.1. The maximum deflection at the centre was 73.7 mm and at the L/4 of effective span the deflection was 31.3mm. The values of deflection with successive load are shown in the Table 4.1

**Table – 4.1 Detail of Load v/s Deflection of Control Beam 01 (FDB 01)**

| Load (KN) | Deflection (L/2) (mm) | Deflection (L/4) (mm) |
|---|---|---|
| 0 | 0 | 0 |
| 4 | .52 | .1 |
| 8 | 1.21 | .51 |
| 12 | 1.98 | .84 |
| 16 | 2.89 | 1.33 |
| 20 | 4.03 | 2.01 |
| 24 | 5.37 | 2.87 |
| 28 | 6.81 | 4.09 |
| 32 | 8.11 | 5.23 |
| 36 | 9.38 | 6.12 |
| 40 | 10.31 | 6.93 |
| 44 | 11.46 | 8 |
| 48 | 12.52 | 9.18 |
| 52 | 13.64 | 9.94 |
| 56 | 14.89 | 10.59 |
| 60 | 16.05 | 11.61 |
| 64 | 17.82 | 12.6 |
| 68 | 19.05 | 13.63 |
| 72 | 20.54 | 14.7 |
| 76 | 22.45 | 15.37 |
| 80 | 27.47 | 16.84 |
| 84 | 35.62 | 18.81 |
| 88 | 45.51 | 21.41 |
| 90 | 48.89 | 22.89 |
| 91 | 55.63 | 24.27 |
| 92 | 61.53 | 26.12 |
| 93 | 66.16 | 27.98 |
| 94.9 | 73.77 | 31.29 |

| | | |
|---|---|---|
| 80 | 75.27 | 33.15 |

**Fig-4.1 Crack Pattern of Control Beam 01 (FDB 01)**

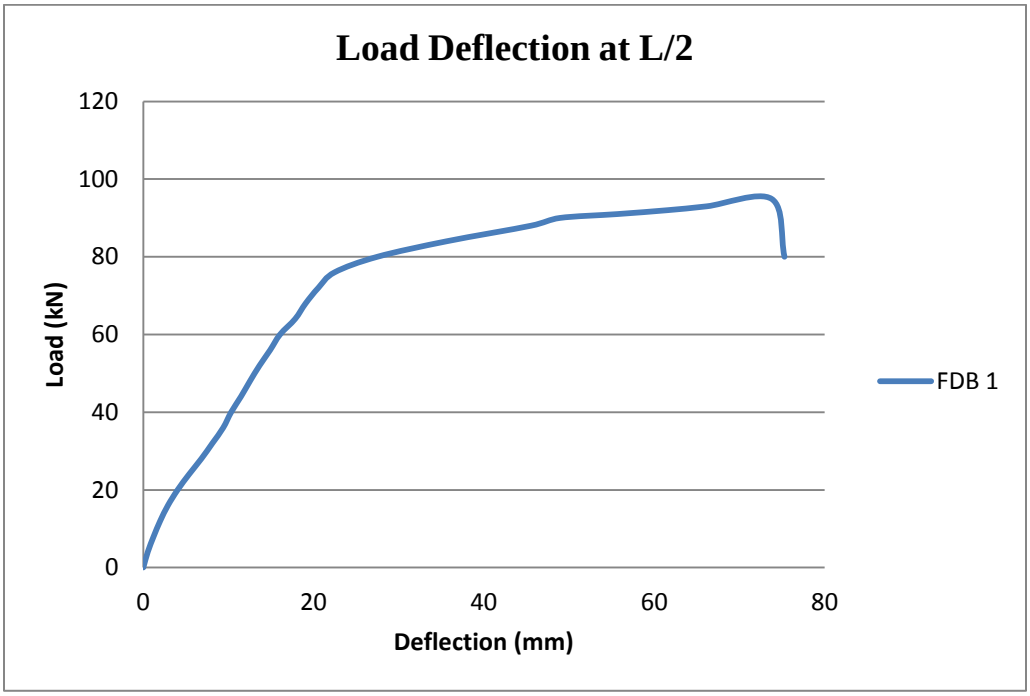


**Fig- 4.2 Load v/s Mid Span Deflection of Controlled Beam 01 (FDB 01)**

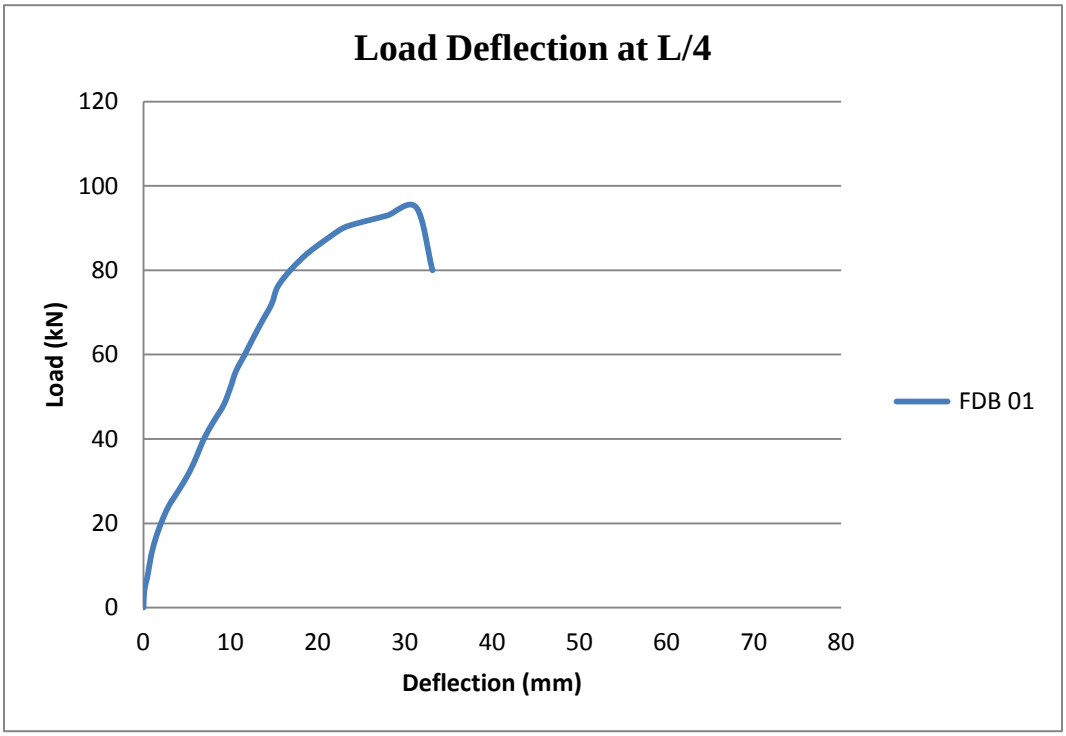


**Fig- 4.3 Load v/s Quarter Span Deflection of Controlled Specimen (FDB 01)**

(FDB 02) is the another controlled sample which was tested for preparing the load deflection graph.Values of load deflection graph is shown in Table 4.2 below.

**Table no – 4.2 Detail of Load v/s Deflection of Control Beam (FDB 02)**

| Load (KN) | Deflection (L/2) (mm) | Deflection (L/4) (mm) |
|---|---|---|
| 0 | 0 | 0 |
| 4 | .61 | .23 |
| 8 | 1.34 | .62 |
| 12 | 2.07 | 1.21 |
| 16 | 3.53 | 2.09 |
| 20 | 4.83 | 2.97 |
| 24 | 6.21 | 3.93 |
| 28 | 7.98 | 5.36 |
| 32 | 9.62 | 6.24 |

| | | |
|---|---|---|
| 36 | 10.84 | 6.94 |
| 40 | 12.08 | 8.18 |
| 44 | 13.21 | 9.03 |
| 48 | 14.05 | 9.69 |
| 52 | 14.94 | 10.56 |
| 56 | 16.41 | 11.37 |
| 60 | 17.72 | 11.68 |
| 64 | 19.13 | 12.61 |
| 68 | 20.92 | 13.58 |
| 72 | 22.13 | 15.81 |
| 76 | 27.26 | 17.76 |
| 80 | 33.11 | 20.37 |
| 84 | 38.48 | 22.28 |
| 88 | 47.96 | 24.51 |
| 90 | 52.53 | 26.43 |
| 91 | 58.51 | 28.73 |
| 92 | 62.86 | 30.13 |
| 93.8 | 69.85 | 33.15 |
| 85 | 72.13 | 33.61 |

**Fig –4.4 Crack Pattern of Controll Specimen 02 (FDB 02)**

Beam “FDB 02” was identical as like the previous one “FDB 01” .The load deflection graph was prepared by the software untill the beam failed.The hair line cracks obtained in the flexural region in the intial stage of incresing load.The first crack occurred at 51 kN at the centre region, consecutively with the increasing load more cracks were observed. Second crack was observed at 67 kN at below right point load. As load reached at 70 kN more cracks were observed. At the stage of 84 kN, from the curve it is analyzed that yielding of steel has started. At 93.8 kN beam has stopped taking further load. The maximum deflection at the center was 69.85 mm and at L/4 was 33.15 mm.At the end of experiment it could be clearly seen that the maximum deflection obtained at the centre. All subcracks were concted with the major cracks.The load deflection graph at a distance of L/2 and at L/4 are shown in figure 4.5 and figure 4.6.

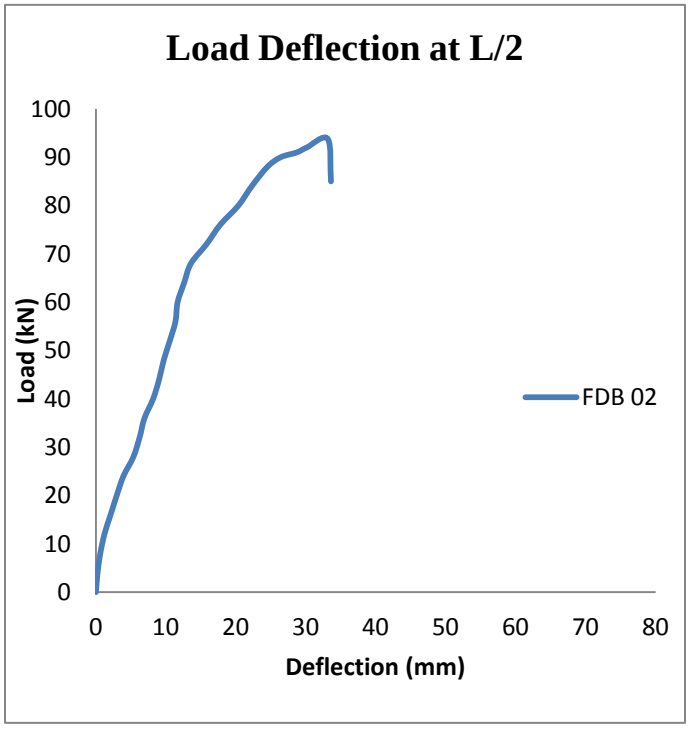


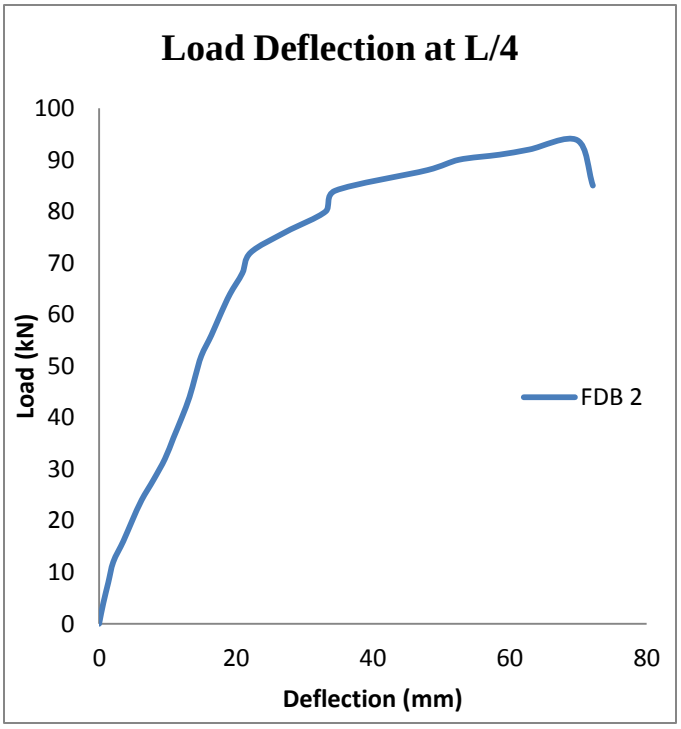


**Fig–4.5 Load v/s Mid Span Deflection of Control Beam 02(FDB 02)**

**Fig-4.6 Load v/s Quarter span Deflection of Controll Beam 02 (FDB 02)**

## 4.3 Average Load Deflection Graph of Controlled Specimens

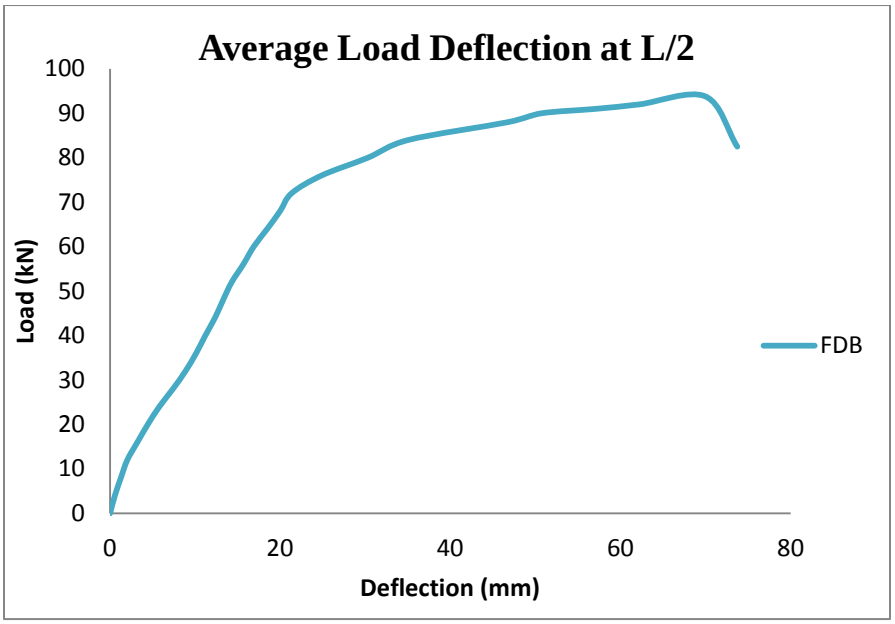


**Fig-4.7 Average Load v/s Mid Span Deflection of Control Beam (FDB)**

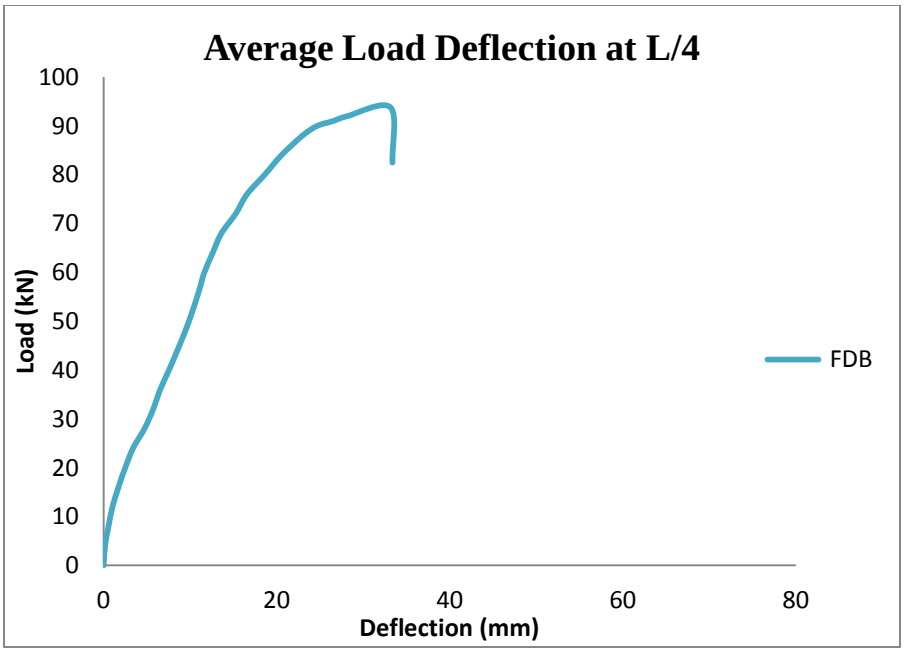


**Fig- 4.8 Average Load v/s Quarter span Deflection of Control Beam (FDB)**

The purpose of preparing the average load deflction graph of controlled specimen is to establishing a remarkable identification for taken out the stages,described below. Afterwards of 78 kN elasto- plastic stage has been observed.Prior to that beam was in elastic stage. At the reach

of 91 KN beam behaviour transformed to plastic zone. At the load of 94.35 KN beam has stopped taking further load .

### 4.3.1 Elastic State

From average load deflection of controlled specimen,range of elastic state has identified. At a state 0% to 82.7% of ultimate load the behaviour of beam was elastic.

### 4.3.2 Elasto Plastic State

This stage sustained during testing from 82.7% to 96.5% of ultimate load.

### 4.3.3 Plastic State

The plastic stage began afterwards of 96.5% of ultimate load.

## 4.4 Effect of Prestress level on Retrofitted Beams Strength Parameter

Four beams were retrofitted with different prestressed level.The beams were retrofitted with different prestressing force. The beams were damaged fully prior to retrofit. The detailed results of each category are described below.

- Two beams retrofitted with 60% force of ultimate tensile load (UTL) of CFRP
- Two beams retrofitted with 80% force of ultimate tensile load (UTL) of CFRP

### 4.4.1 Beams Retrofitted with 60 % prestressing of CFRP

#### 4.4.1.1 01 RDB60

Two beams were retrofitted with 60% of ultimate tensile load of CFRP sheet.81 kN force was applied for prestressing the CFRP sheet and corresponding to above force, the required elongation was 30mm.The required force was applied by jack and corresponding elongation was measured by LVDT. The instant effect of prestressing on initially damaged beam during prestressing were observed by LVDT, which was placed at the centre. Previous cracks were opened at 57 kN. At 72 kN new cracks occurred below the left point load.The second crack was occurred at 84 kN under the left point load.Third crack observed at 92 kN between the left point load and the center. with the increment of load, more number of cracks were observed at mid span and then connected with the major cracks. At a load value of 98 kN fiber was started to fracture .It was observed that CFRP sheet was not fracture in transverse as well as in longitudnal

at once. Sheet was fractured strip by strip, loud sound of CFRP strip frecture heard at 103 kN. At a load value of 116 kN the second strip of fiber was frecture and loud sound of beam cracking was heard. The CFRP sheet fracture in transverse direction at the load of 126.72 kN, at this stage beam has stopped taking load.The maximum deflection at the centre is 36 mm an at L/4 is 25.76. Fig 4.9 shows the crack pattern and 4.10 shows the fiber frecture of specimen. It has been observed that in the case of retrofitted beams, 72 % safe load increased as compared to control beams.

**Fig –4.9 Crack Pattern of 01 RDB60**

**Fig- 4.10 Fiber Fracture 01 RDB60**

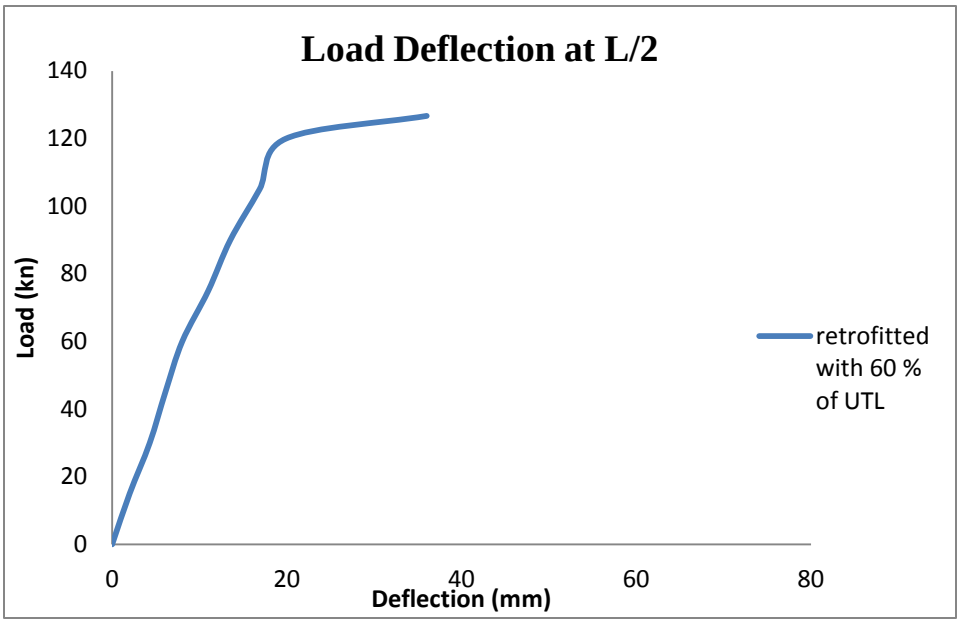


**Fig-4.11 Load vs Mid Span Deflection of Retrofitted Beam with Prestressed CFRP Sheet (60% UTL)**

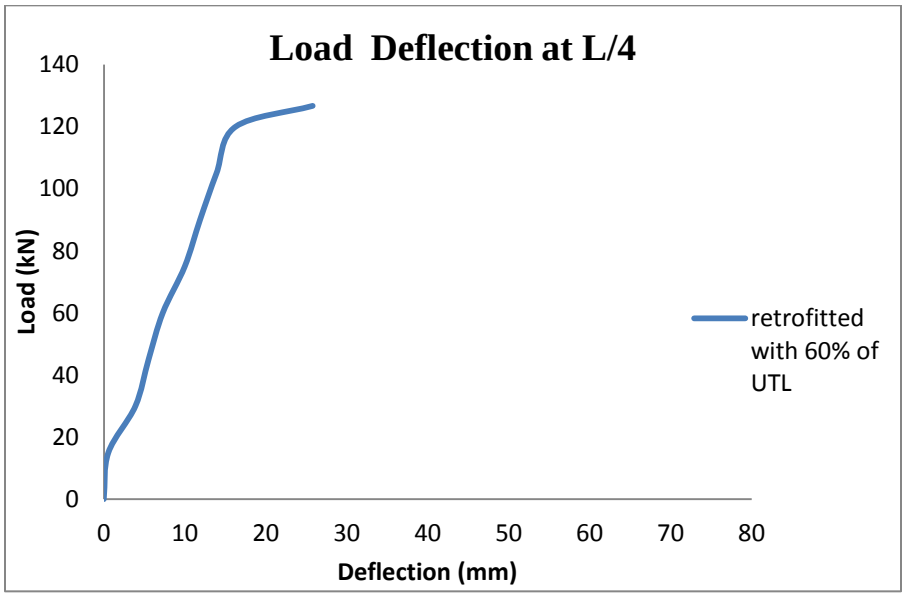


**Fig- 4.12 Load vs Quarter Span Deflection of Retrofitted Beam With Prestressed Fiber Sheet (60% UTL)**

### 4.4.1. 2 02 RDB60

The beam has an identical behaviour as like 01 RDB60. The first crack was occured at 73 KN between the left point load and the center of beam. It propagate towards upside with the incresing load. The fiber fractured finally followed by debonding. First fiber strip was frectured at 104 kN. Fiber failure by fracture increasing with the increasing load. Finally at 126 kN beam stopped taking load.Fig 4.13 shows the crack pattern and fig 4.14 shows the CFRP failure of 02 RDB 60.

**Fig-4.13 Crack Pattern of Retrofitted Beam with presstressing of 60% UTL of CFRP Sheet**

**Fig–4.14 Fiber Frecture Faliure of Retrofitted Beam with presstressing of 60% UTL of CFRP Sheet (02 RDB 60)**

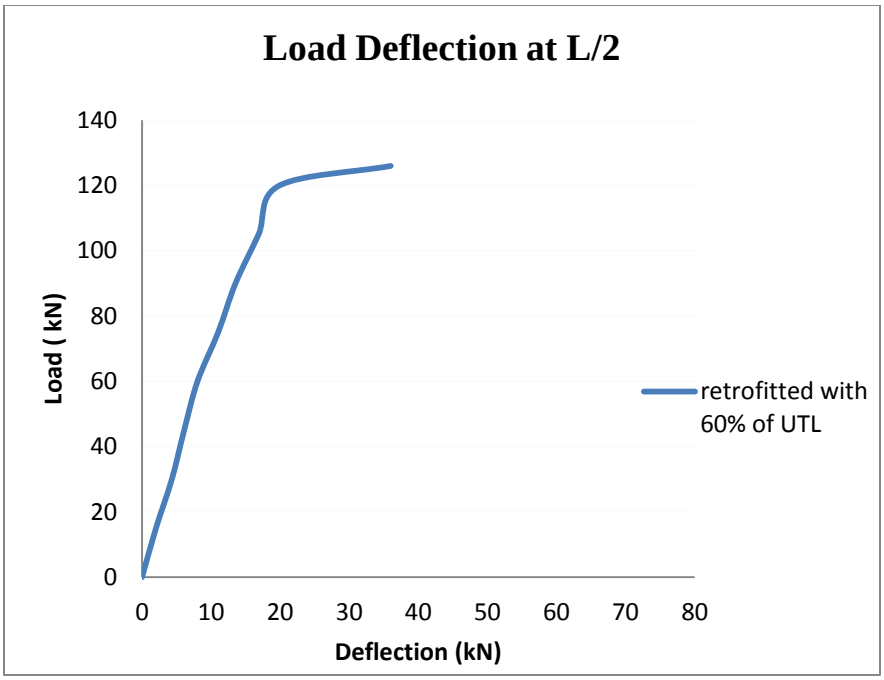


**Fig-4.15 Load vs Mid Span Deflection of Retrofitted Beam with presstressing of 60% UTL of CFRP Sheet (02 RDB60)**

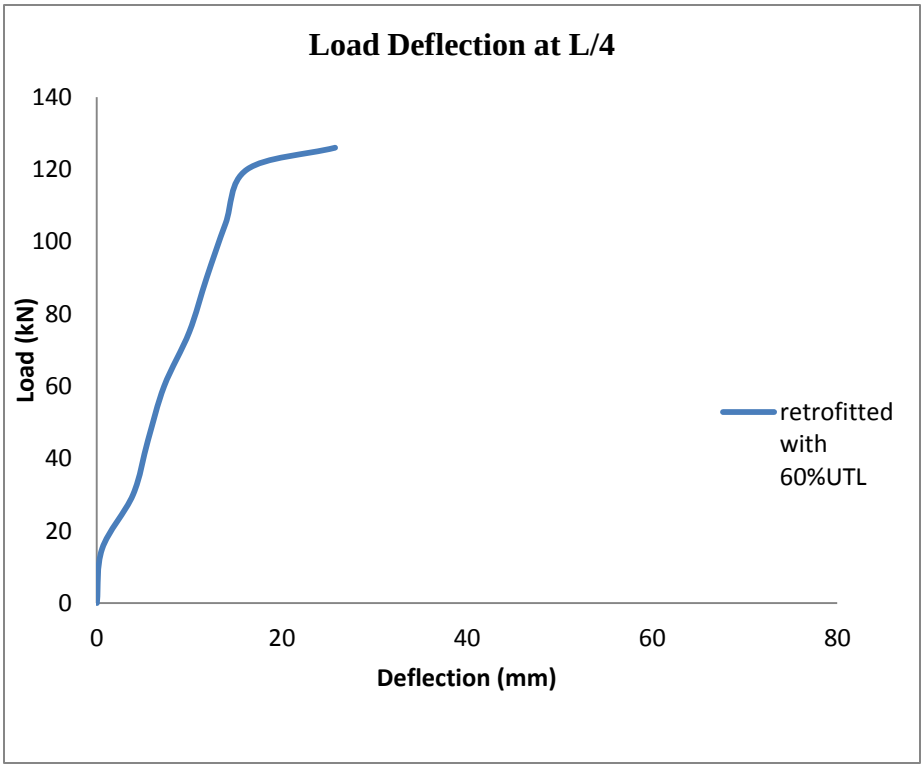


**Fig-4.16 Load vs Quarter Span Deflection of Retrofitted Beam with presstressing of 60% UTL of CFRP Sheet**

### 4.4.2 Beams Retrofitted with 80% Prrestressing of CFRP

#### 4.4.2.1 01 RDB80

80% of ultimate tensile load of CFRP was used for the retrofitting of intially damaged beam.It was observed that the ultimate load carrying capacity of retrofitted beam under this category more as compared to other specimens.During testing new cracks occured at 99 kN which was at the mid span of specimen.The second crack was occurred in between the left point load and midspan, third crack came near to the right of midspan.The previous cracks propagate and opened more towards upside under the point load.The observed crack pattern is showing below in a figure 4.17. Fiber fracture at 113 kN longitudnally as well as transversally in a form of small strips. Figure 4.18 below showing the failuer of fiber by fracture.Second small fiber strip fracture at 121 kN.Third and fourth fiber was ruptured at 133 kN and 140 kN.The beam has stoped taking load at 146.61 kN.The safe load of prestressed retrofitted beam has been increased by 72% as compared to controlled beam.

**Fig- 4.17 Crack Pattern of Retrofitted Beam with presstressing of 80% UTL of CFRP Sheet (01 RDB80)**

**Fig- 4.18 Fiber Failure by Frecture of Retrofitted Beam with presstressing of 80% UTL of CFRP Sheet (01 RDB80)**

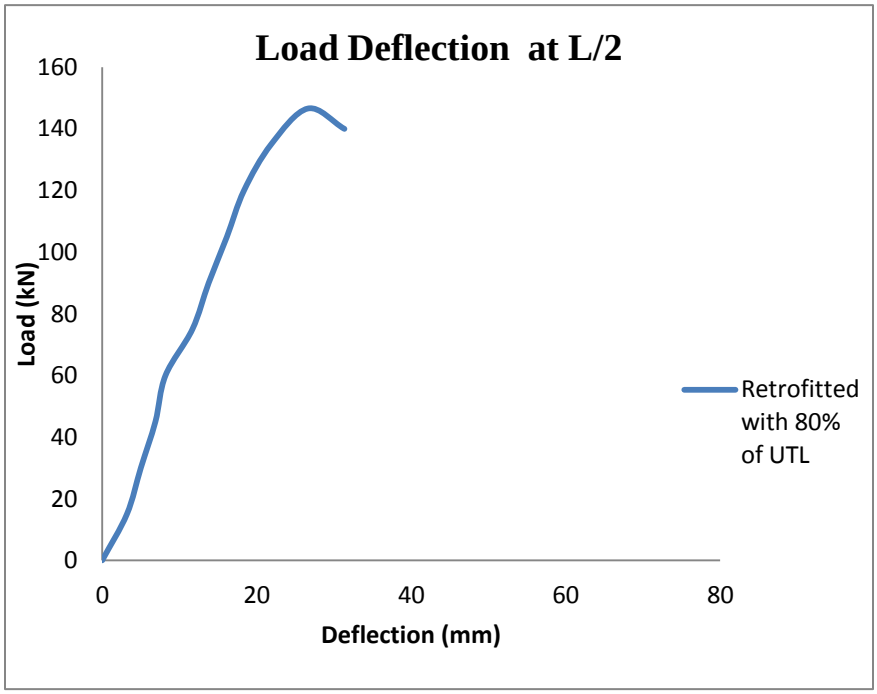


**Fig–4.19 Load vs Mid Span Deflection of Retrofitted Beam with presstressing of 80% UTL of CFRP Sheet (01 RDB80)**

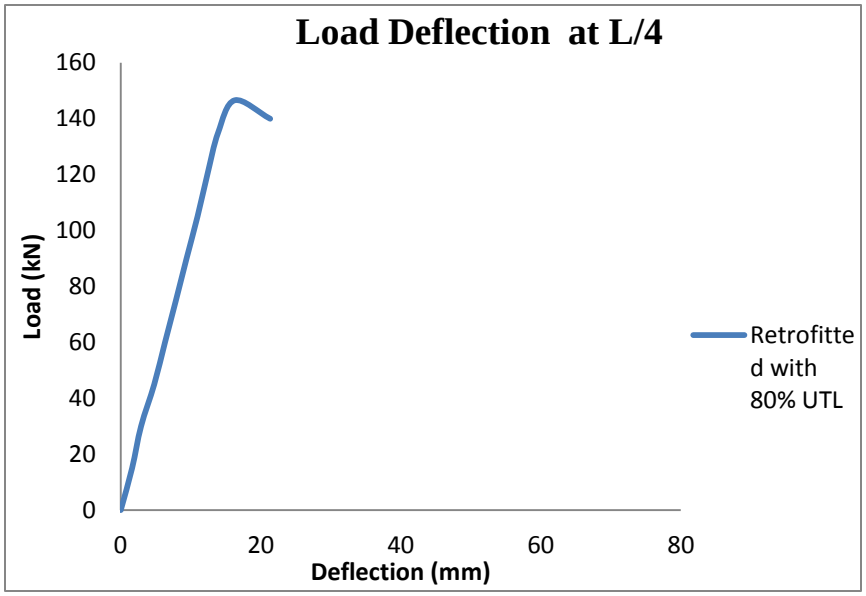


**Fig –4.20 Load vs Quarter span Deflection of Retrofitted Beam with presstressing of 80% UTL of CFRP Sheet (01 RDB80)**

### 4.4.2.2 02 RDB 80

The deflection observed in this specimen was more as compared to 01RDB 80. Prestressed fiber sheet was failed by frecture failure followed by peeling of fiber sheet in the strip from the surface.The maximum deflection was observed 44.86 mm at the center and 30 mm at L/2. First crack was observed at the mid span at 107 kN and Propagate vertically upward .Nearby right side of mid span second crack was propagate at 119 kN.The third crack occurd under the right side of point Load at 127 kN.The more cracks observed as load was increased.After the failure of fiber at 150 kN, the cracks started widend and yielding of steel takes place.

**Fig- 4.21 Crack Pattern of Retrofitted Beam with presstressing of 80% UTL of CFRP Sheet (02 RDB80)**

**Fig-4.22 Fiber Failure by Frecture of Retrofitted Beam with presstressing of 80% UTL of CFRP Sheet (02 RDB80)**

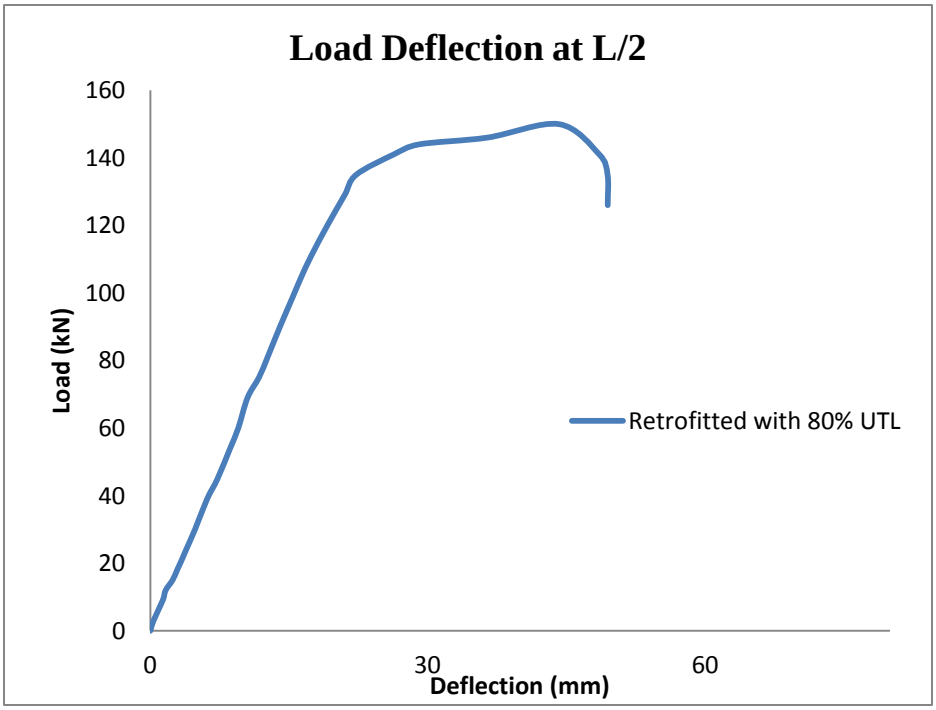


**Fig–4.23 Load vs Mid Span Deflection of Retrofitted Beam with presstressing of 80% UTL of CFRP Sheet (02 RDB80)**

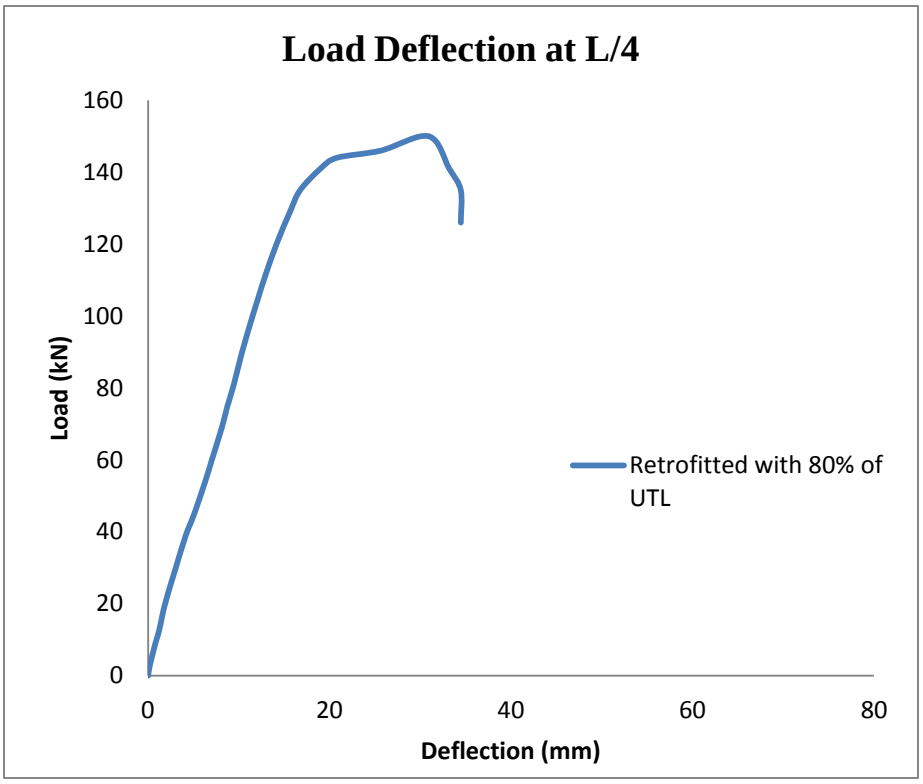


**Fig- 4.24 Load vs Quarter Span Deflection of Retrofitted Beam with presstressing of 80% UTL of CFRP Sheet (02 RDB80)**

## 4.5 Comparison of Controlled Beam with Retrofitted Beams

After the experimental work, there is a distinct diffrence in the load carrying capacity of controlled and retrofitted specimens. The load carying capacity of beam was improved as method of retrofitting transformed from non prestressed to prestressed CFRP. From the Figure 4.25, [1] (non prestressed single layer of CFRP sheet) increased the load carying capacity of beam as compared to controll beam.The 60% prestressed beam has shown linear behaviour upto 120 kN althought sheet was started to fractured strip by strip at 103 kN. Beyond the 120 kN the fractured failure was started in the CFRP sheet and the plastic zone came into the picture. It has shown that the beam was not failed by brittle manner. By single layer of prestressed sheet the ultimate strength of fiber sheet was utilized (because fracture failure occure). The safe load for the retrofitted beam has been increased by 72% as compare to the controll beam. During the

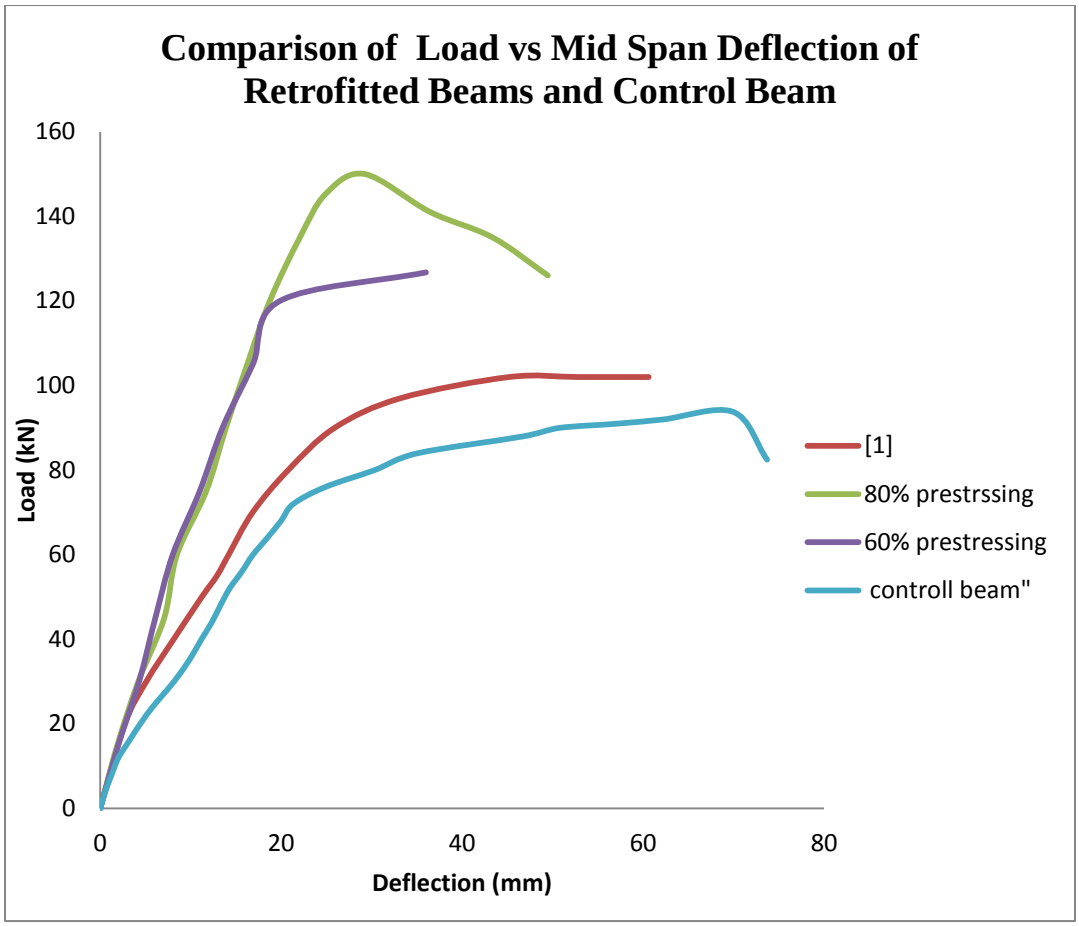


**Fig-4.25 Comarison of Load vs Mid Span Deflection of Retrofitted Beams with Control Beam**

prestressing of CFRP the deflection of beam was arrived back to upward side.The recovery of deflection leads to the increment of residual resistance also in beam. The Increment of prestressing magnitude from 60 to 80 %, the load carying capacity of specimen simultaneously increased.The curve was linear upto 140 kN load in the case of 80% prestressed single layer .

As the number of prestressed CFRP layer has increased, the failure transformed from fiber frecture to debonding[2]. The significant conclusion from the experimental study is that as go on increasing the number of layer, it does not mean that the ultimate strength of specimen will also increased. it increased upto some extent but beyond that debonding can occurred. Table 4.3 below shows the brief observations during the experimental study.

**Table-4.3 Brief Observation During Experiment**

| Beam state | No of CFRP sheet | Ultimate load (KN) | Type of CFRP failure |
|---|---|---|---|
| Control beam (FDB 01) (FDB 02) | ---- | 94.35 | ---- |
| Single non prestressed sheet [1] | 1 | 102.3 | Fracture |
| Retrofitted beam (01 RDB60) | 1 | 126.72 | Fracture |
| Retrofitted beam (02RDB 60) | 1 | 126 | Fracture |
| Retrofitted beam (01RDB 80) | 1 | 146.61 | Fracture |
| Retrofitted beam (02RDB 80) | 1 | 150 | Fracture |

## 4.6 Comperison of Stiffness Between Control and Retrofittted Specimens

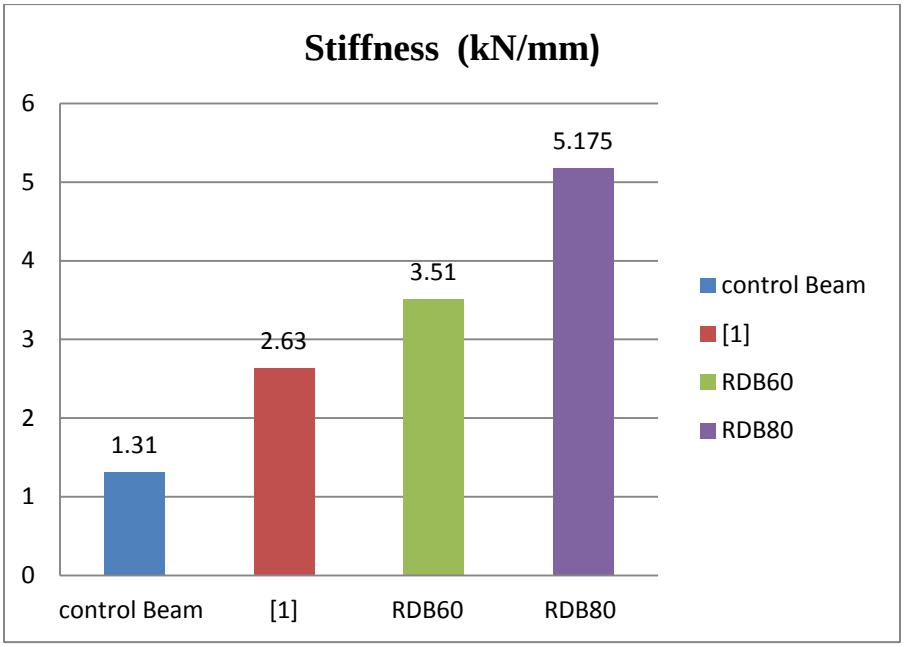


**Fig- 4.26 Stiffness Variation of Specimens**

The fig 4.26 shows the variation of stiffness with respect to the control and retrofitted beams.The maximum stiffness was observed in the retrofitted specimen prestressed by 80% of UTL of CFRP sheet . Due to failure of CFRP in fracture mode ,it was utilized its ultimate tensile strength.The average stiffness of RDB60 is 3.51 kN/mm.The failure in this case was also in fracture mode.The effective utilization of the CFRP tensile strength depends upon the prestressing magnitude. The single layer non prestressed sheet [1] failed in fracture mode but the load carying capacity was 32% decreases as compared to RDB80. It means that with the prestressing of single layer CFRP the performance of sheet as well as specimens both improved up to certain limit. Sheet improved its performance by debonding to fracture failure and concrete specimen improved its mode of failure from brittle to ductile. After the experimental study, it has been observed that stiffness as well as number of CFRP layers transform the mode of failure. With the increment of CFRP layers during retrofitting, it directly increase the load carying capacity of specimen up to some extent but the ultimate strength of CFRP is not utilized.

## Conclusion

The results obtained under this experimental study have shown a conclusion in the field of retrofitting of reinforced concrete structure.The prestressing of CFRP enhanced the structure performance and it is better feasible option than other method.The maximum strength utilization of CFRP have utmost significance.Now researchers are moving towards the effective and maximum utilization of CFRP.The following conclusion drawn from the experimental study shown below.

1. The Single layer prestressed CFRP sheet perform well in the case of efective utilization of tensile strength of CFRP.
2. The 58.98% load carying capacity increased as compared to controlled specimen by the application of Single layer pretressed CFRP sheet with 80% prestressing force.
3. The 33.54% load carying capacity increased as compared to controlled specimen by applying the single layer prestressed CFRP with 60% prestressing force.
4. The safe load for the RDB80 and RDB60 incressed by 72% as compared to controlled specimen.it is incresed due to the stiffness imposed by CFRP at the tension face of Retrofitted beam.
5. With the increment of prestressing force, deformation in the perpendicular direction of specimen laid was reduced subsequently. The results shows that the controlled specimen have maximum deflection, on the other side the minimum deflection showed by RDB80 specimen .This was only due to the stiffness convey by the CFRP at the tension side.
6. It was observed that the more load required to transferred the crack from tension to compression side of the beam in the retrofitted beam as compared to controlled specimens.Increased deformation resistance observed in the retrofitted beam due to the prestressed CFRP sheet.

## References


1. Gill.H.,S,(2009)"Retrofitting of RC Beams by Prestressing Fibers"Dessertation Report,Thapar University,
2. Mehta.A, (2011) "Effect of Initial Stress Levels on Strength of Beams Retrofitted Using Pre-Stressed Fibre Composites" Dessertation Report,Thapar University,
3. Obaidat.Y.,T, Heyden.S, Dehlblom.O, Farsakh.A.,G, Jawad.A.,Y, (2011) "Retrofitting of Reinforced Concrete Beams using Composite Laminaes." Construction and Building Materials,Vol 25, pp 591-597.
4. Mukherjee.A, Rai.G.,L, (2008)"Performance of Reinforced Concrete Beams Externally Prestressed with Fiber Composites."Construction and Building Materials,pp 591-597.
5. Rusinowski.P,Taljasten.B,(2007)"Interlaminar Peeling in Concrete Beams Strengthenened with CFRP Plates-Experimental Study"International Institute for FRP in Construction" Asia Pacific Confrence on FRP in Structures.
6. Sharma.K.,S, Ali.M.,S, Goldar. D., Sikdar. P.,K,(2006) " Plate-Concrete Interfacial Bond Strength of FRP and Metallic Plated Concrete Specimens" Composites Engineering,Vol 37,pp 54-62.
7. Teng.J.,G, Smith.S.,T, Yao.J, Chen.J.,F,(2003) "Intermediate crack-Induced Debonding in RC Beams and Slabs" Construction and Building Materials,Vol 17, pp 447-462.
8. Saadamanesh.H,Ehasani.R.,M,(1991) "RC Beams Strengthened with GFRP Plates" Journal of Structural engineering"Vol 117.
9. Aiello.M.,A, Ombres.L,(2000)"Load-Deflection Analysis of FRP Reinforced Concrete Flexural members" Journal of Composits of Construction,Vol 4,PP 164-171.
10. Mukherjee.A, Bagadi.S.,P, Rai.G.,L, (2009) "Semianalytical Modeling of Concrete Beams Rehabilitated with Externally Prestressed Composites" Journal of Composites for Construction,Vol 13.
11. Teng.J.,G,Yuan.H,Chen.J.,F,(2006) "FRP to Concrete Interface Between Two Adjacent Cracks:Theoretical Model for Debonding Failure" International Journal of Solids and Structures"Vol 43,PP 5780-5778.
12. Mukherjee.A,Boothby.T.,E,Bakis.C.,E,Joshi.M.,V,Maitra.S.,R,(2004)"mechanical Behaviour of Fiber-reinforced Polymer-Wrapped Concrete Columns-Complicating Effects" Journal of Composits of Construction,Vol 8,PP 97-103.

13. Abdelrahman.K,Hacha.R,(2012) “Size Effect Study of CFRP and SFRP Wrapped Concrete Specimens”
14. Bisbay.L,Li.S,Duerden.B,Mclarty.K,Chen.J.,F,Stratford.T, “Effects of Unconfined Concrete Strength on FRP Confinement of Concrete”
15. Atmur.S.,D,(1998)“Compression Injection Modling of Polymer-Derived Fiber Reinforced Cramic Matrix Composites Material”United State Patient.
16. Teng.J.,G,Yu.T, Fernando.D., “Strengthening of steel structures with fiber-reinforced polymer composites” Journal of Constructional Steel Research, Vol 78,PP 131-143.
17. Raju.A, Mathew. L., A,(2013) “Retrofirring of RC Beams using FRP” International Journal of Engineering Research & Technology (IJERT), Vol 2.
18. B.Oral, Gunes. O, Karaca. E, (2004) “ Progress on understanding debonding problems in reinforced concrete and steel members strengthened using FRP composites”Construction and Building Materials,Vol 19, PP 9-19